EFFECTS OF ATMOSPHERIC PATH ON AIRBORNE MULTISPECTRAL SENSORS

Robert Horvath
John G. Braithwaite
Fabian C. Polcyn

January 1969

Prepared Under NASA Grant NsG 715/23-05-071 by
INFRARED AND OPTICAL SENSOR LABORATORY
WILLOW RUN LABORATORIES
INSTITUTE OF SCIENCE AND TECHNOLOGY
THE UNIVERSITY OF MICHIGAN
Ann Arbor, Michigan

NATIONAL AERONAUTICS AND SPACE ADMINISTRATION

FOREWORD

This report is one of several in a program to determine the feasibility of developing an imaging sensor which uses the spectral characteristics of a scene point to identify materials of interest or to enhance the contrast of selected objects. Multispectral imagery and video data are being generated over scenes of interest from an airborne platform. Multiband images are analyzed and interpreted using conventional photointerpretation techniques, and the spectral characteristics of targets and background objects are analyzed to determine how to electronically process the spectral information from a scene in real time for improved remote sensing. The general goal of this program is to develop methods of improving and extending current aerial-survey capabilities; improvements are sought in the kinds and quantity of data obtainable and in the quality and economy of imagery interpretation.

This multispectral program was initiated and is being guided by Marvin R. Holter, Head of the Infrared and Optical Sensor Laboratory of Willow Run Laboratories, a unit of the University of Michigan's Institute of Science and Technology. Previous reports issued by the Infrared and Optical Sensor Laboratory under this and related programs are given in the list of related reports which immediately follows.

The work reported herein was sponsored by the National Aeronautics and Space Administration under Grant NsG715/23-05-071, "The Investigation of a Method for Remote Detection and Analysis of Life on a Planet." Contractor's number for this report is 1674-5-T. The Principal Investigator for this research is D. S. Lowe, Head of the Sensor Systems Group of the Infrared and Optical Sensor Laboratory. Contributions to this report in addition to those of the authors were made by W. Brown, P. Hasell, and L. Munford.

RELATED REPORTS

COMPARATIVE MULTISPECTRAL SENSING (U), M. R. Holter and F. C. Polcyn, Report No. 2900-484-R, Willow Run Laboratories of the Institute of Science and Technology, The University of Michigan, Ann Arbor, June 1965, AD 362 283 (CONFIDENTIAL).

DIURNAL AND SEASONAL VARIATIONS IN RADIATION OF OBJECTS AND BACKGROUNDS, 4.5-5.5-μ SPECTRAL REGION (U), L. D. Miller and R. Horvath, Report No. 6400-32-T, Willow Run Laboratories of the Institute of Science and Technology, The University of Michigan, Ann Arbor, June 1965, AD 362 620 (CONFIDENTIAL).

THE INVESTIGATION OF A METHOD FOR REMOTE DETECTION AND ANALYSIS OF LIFE ON A PLANET, M. R. Holter, D. S. Lowe, and R. J. Shay, Report No. 6590-1-P, Institute of Science and Technology, The University of Michigan, Ann Arbor, November 1964.

SPECTRUM MATCHING (U), R. E. Hamilton, Report No. 6400-18-T, Willow Run Laboratories of the Institute of Science and Technology, The University of Michigan, Ann Arbor, June 1965, AD 363 001 (CONFIDENTIAL).

TARGET SIGNATURE STUDY, INTERIM REPORT, VOLUME I: SURVEY (U), R. R. Legault and T. Limperis, Report No. 5698-22-T(I), Institute of Science and Technology, The University of Michigan, Ann Arbor, October 1964, AD 354 166 (CONFIDENTIAL).

TARGET SIGNATURE STUDY, INTERIM REPORT, VOLUME II: RECOMMENDATIONS (U), R. R. Legault and T. Limperis, Report No. 5698-22-T(II), Institute of Science and Technology, The University of Michigan, Ann Arbor, October 1964 (CONFIDENTIAL).

TARGET SIGNATURE STUDY, INTERIM REPORT, VOLUME III: POLARIZATION (U), R. R. Legault and T. Limperis, Report No. 5698-22-T(III), Institute of Science and Technology, The University of Michigan, Ann Arbor, October 1964, AD 354 025 (CONFIDENTIAL).

TARGET SIGNATURE STUDY, INTERIM REPORT, VOLUME IV: BIBLIOGRAPHY (ACOUSTIC, ULTRAVIOLET, VISIBLE, INFRARED, AND RADAR) (U), T. Limperis and R. S. Gould, Report No. 5698-22-T(IV), Institute of Science and Technology, The University of Michigan, Ann Arbor, October 1964, AD 354 232 (SECRET).

TARGET SIGNATURE STUDY, INTERIM REPORT, VOLUME V: CATALOG OF SPECTRAL REFERENCE DATA, R. R. Legault, R. S. Gould, and T. Limperis, Report No. 5698-22-T(V), Institute of Science and Technology, The University of Michigan, Ann Arbor, October 1964.

A COMPREHENSIVE TARGET-SIGNATURE MEASUREMENT PROGRAM, FIRST INTERIM TECHNICAL REPORT, VOLUME I: TECHNICAL DISCUSSION (U), Report No. 7251-3-P(I), Willow Run Laboratories of the Institute of Science and Technology, The University of Michigan, Ann Arbor, December 1965 (CONFIDENTIAL).

A COMPREHENSIVE TARGET-SIGNATURE MEASUREMENT PROGRAM, SECOND INTERIM TECHNICAL REPORT, VOLUME I: DATA PROCESSING, STORAGE, AND ANALYSIS (U), Report No. 7251-9-P(I), Willow Run Laboratories of the Institute of Science and Technology, The University of Michigan, Ann Arbor, June 1966 (CONFIDENTIAL).

A COMPREHENSIVE TARGET-SIGNATURE MEASUREMENT PROGRAM, SECOND INTERIM TECHNICAL REPORT, VOLUME II: MEASUREMENT IMPLEMENTATION (U), Report No. 7251-9-P(II), Willow Run Laboratories of the Institute of Science and Technology, The University of Michigan, Ann Arbor, June 1966 (CONFIDENTIAL).

A COMPREHENSIVE TARGET-SIGNATURE MEASUREMENT PROGRAM, THIRD INTERIM TECHNICAL REPORT (U), Report No. 7251-15-P, Willow Run Laboratories of the Institute of Science and Technology, The University of Michigan, Ann Arbor, February 1966 (CONFIDENTIAL).

A COMPREHENSIVE TARGET-SIGNATURE MEASUREMENT PROGRAM, FINAL REPORT (U), T. Limperis, Report No. 7251-21-F, Willow Run Laboratories of the Institute of Science and Technology, The University of Michigan, Ann Arbor, December 1966, AD 378 112 (CONFIDENTIAL).

DISPERSIVE MULTISPECTRAL SCANNING: A FEASIBILITY STUDY, FINAL REPORT, J. Braithwaite, Report No. 7610-5-F, Willow Run Laboratories of the the Institute of Science and Technology, The University of Michigan, Ann Arbor, September 1966.

AN INVESTIGATIVE STUDY OF A SPECTRUM-MATCHING IMAGING SYSTEM, FINAL REPORT, D. S. Lowe, J. Braithwaite, and V. L. Larrowe, Report No. 8201-1-F, Willow Run Laboratories of the Institute of Science and Technology, The University of Michigan, Ann Arbor, October 1966.

TARGET SIGNATURES ANALYSIS CENTER: DATA COMPILATION, D. G. Earing and J. A. Smith, Report No. 7850-2-B, Willow Run Laboratories of the Institute of Science and Technology, The University of Michigan, Ann Arbor, July 1966, AD 489 968.

OPTICAL SENSING OF MOISTURE CONTENT IN FINE FOREST FUELS, FINAL REPORT, C. E. Olson, Jr., Report No. 8036-1-F, Willow Run Laboratories of the Institute of Science and Technology, The University of Michigan, Ann Arbor, May 1967.

TARGET-SIGNATURE MEASUREMENTS, FIRST INTERIM REPORT (U), Report No. 8047-7-P, Willow Run Laboratories of the Institute of Science and Technology, The University of Michigan, March 1967 (CONFIDENTIAL).

THE INVESTIGATION OF A METHOD FOR REMOTE DETECTION OF LIFE ON A PLANET, L. D. Miller, Report No. 6590-4-F, Willow Run Laboratories of the Institute of Science and Technology, The University of Michigan, Ann Arbor, November 1965.

INVESTIGATIONS OF SPECTRUM MATCHING SENSING IN AGRICULTURE (U), F. Polcyn and W. A. Malila, Report No. 6590-7-P, Willow Run Laboratories of the Institute of Science and Technology, The University of Michigan, Ann Arbor, September 1967 (Vol. I: UNCLASSIFIED; Vol II: CONFIDENTIAL).

ABSTRACT

Experimental data have been acquired for a study of the effects of variable atmospheric path on the spectral signals obtained by remote sensors in the optical region of the spectrum. Multichannel optical-mechanical scanners which provide calibrated apparent spectral radiance data were flown over agricultural test sites, and passes were made at several different altitudes between 2000 and 10,000 ft. The quantitative results compare favorably with qualitative theoretical predictions. Optical-mechanical scanners and aerial photographic systems are compared to show the relative importance of potentially detrimental atmospheric path effects with regard to the operation of these systems in remote sensing.

CONTENTS

FIGURES

EFFECTS OF ATMOSPHERIC PATH ON AIRBORNE MULTISPECTRAL SENSORS

1 INTRODUCTION

Investigators in the field of remote sensing have long been concerned with the effects of altitude on the data acquired. This has been especially true since high-altitude aircraft and satellite platforms have become available. Historically, the initial (and so far the greatest) emphasis has been on understanding the manner in which increasing atmospheric path lengths affect the spatial ground resolution attainable with long-focal-length high-resolution camera systems. Even with the advent of optical scanning systems, the emphasis was still on resolution, because classical photointerpretation techniques are based upon the common denominator in all such imagery, geometric shape. Concern with the effects of altitude on the apparent intensity of the radiation emanating from the target has usually been restricted to the question of whether or not enough contrast would be present to allow interpretation of geometric "clues." It has become increasingly apparent in recent years, however, that optimum utilization of remote sensing systems requires use of the information contained in the intensity and spectral character of the radiation sensed. In fact, for many applications, knowledge of the spectral distribution of radiation intensity, or spectral signature, of the object viewed can facilitate identifications or discriminations which would be impossible to make if only the geometric shape were considered. In view of this, it has become increasingly important to understand the effects of variable atmospheric path (resulting from variation in altitude and atmospheric conditions) on spectral signatures. This report presents the results of an exploratory investigation of the effects of altitude on multichannel scanner data. The investigation was limited to those effects relating to the spectral signature problem, but for completeness, the effects of altitude on spatial resolution are also reviewed.

2 THEORETICAL CONSIDERATIONS

2.1. EFFECTS OF ALTITUDE ON SPATIAL RESOLUTION

The spatial resolution of either photographic or optical-mechanical scanner imagery generally has the form of constant angular resolution, so that the linear resolution at the ground is directly proportional to the altitude. (This can, of course, be altered by changing the focal length of the objective lens or mirror and by making other appropriate changes to the equipment.) This involves a simple geometric relation and can readily be accounted for. It is more

important to note that there are less obvious effects which may degrade resolution, but that these are likely to become less important as altitude is increased or are likely to produce a constant degradation of the angular resolution.

The degradation of ground resolution due to scintillation caused by atmospheric turbulence will, for a given atmospheric condition, become less noticeable as the altitude is increased, since, for constant angular resolution, the geometric ground resolution will fall off with altitude. In any case, scintillation effects are likely to be relatively insignificant for most aircraft and satellite applications except, perhaps, for some specialized areas such as oblique photography with very long focal-length lenses. If, however, aircraft-induced turbulence leads to significant scintillation, then the effects become more important, but it is believed that this occurs only in certain regimes of high-speed flight with which most applications need not be concerned.

Aircraft vibration and instability may lead to degradation of resolution resulting from motion of the components of the imaging system during exposure. Usually such vehicular motion is reduced in magnitude as altitude is increased, so that performance degradation with increasing altitude is unlikely. Particular aircraft operating conditions which lead to excessive vibration or instability can usually be avoided.

It is often supposed that haze can lead to degradation of spatial resolution. However, it has been shown by Middleton* and others that this is not the case except perhaps under very special circumstances, such as when a very thin layer of dense fog is almost in contact with the target. As shown by Middleton, the more general and more important effect of haze is to destroy the contrast in the image by the dual action of scattering radiation reflected or emitted by the target out of the beam and scattering radiation from any other source into the beam.

2.2. EFFECTS OF ALTITUDE ON APPARENT RADIANCE

2.2.1. ALTITUDE EQUATION. The effect of sensor altitude on the apparent radiance of a target at the earth's surface which fills the sensor's instantaneous field of view can be ascribed to two simultaneous processes. The matter in the atmospheric path between the target viewed and the sensor (1) attenuates by absorption or scattering the radiation emanating (by reflection or self emission) from the target, and (2) scatters and emits unwanted radiation into the field of view so that it appears to come from the target. These effects can be shown in equation form as follows: if $N^t_{\Delta\lambda}$ is the actual radiance of the target, t, in a small spectral bandwidth, $\Delta\lambda$, then the apparent radiance, $N^t_{\Delta\lambda,h}$, sensed vertically from the altitude, h, is given by

*W. E. K. Middleton, Vision Through the Atmosphere, University of Toronto Press, 1958, pp. 78-80.

$$N^{t}_{\Delta\lambda,h} = \tau^{p}_{\Delta\lambda,h} N^{t}_{\Delta\lambda} + N^{p}_{\Delta\lambda,h} \tag{1}$$

where $\tau^{p}_{\Delta\lambda,h}$ is the path transmission coefficient which indicates the degree to which the actual target radiance is attenuated, and $N^{p}_{\Delta\lambda,h}$ is the extraneous radiation emitted or scattered by the atmosphere into the beam and collected by the sensor. The path transmission coefficient and path radiance are functions of $\Delta\lambda$, h, and the atmospheric conditions. It is of interest to consider the implications of equation 1 in order to visualize, at least qualitatively, how such an altitude-radiance relationship affects the remote-sensor data. In particular, it would be of interest to know not only how the apparent radiance of a given target is modified, but also how the radiance difference between two (or more) targets is affected.

In order to observe the effect of altitude on a given target's apparent radiance, the relation in equation 1 may be differentiated relative to altitude, producing

$$\frac{\partial}{\partial h}\left(N^{t}_{\Delta\lambda,h}\right) = \left(N^{t}_{\Delta\lambda}\right)\frac{\partial}{\partial h}\left(\tau^{p}_{\Delta\lambda,h}\right) + \frac{\partial}{\partial h}\left(N^{p}_{\Delta\lambda,h}\right) \tag{2}$$

Now $\partial\tau^{p}/\partial h$ has a negative value since the overall transmission of the path decreases as the path length increases. On the other hand, $\partial N^{p}/\partial h$ has a positive value since (except for some unusual circumstances) the amount of radiation scattered or emitted by the atmosphere into the sensor's field of view increases as the amount of matter (atmospheric path) between the sensor and target increases. Consequently, the direction of the net change with altitude of the apparent target radiance will depend upon the relative magnitudes of $\partial\tau^{p}/\partial h$ and $\partial N^{p}/\partial h$ and upon the magnitude of the actual target radiance. For instance, it can be seen that if the actual target radiance, $N^{t}_{\Delta\lambda}$, were quite small, then the positive term $\partial N^{p}/\partial h$ in equation 2 could well dominate, so that the apparent target radiance, $N^{t}_{\Delta\lambda,h}$, would increase with altitude. Conversely, if the actual target radiance were quite large, then the negative term $\partial\tau^{p}/\partial h$ could well dominate, thus producing a decrease in apparent radiance with altitude.

The radiance difference between two targets, a and b, of actual radiance $N^{a}_{\Delta\lambda}$ and $N^{b}_{\Delta\lambda}$, respectively, is given by

$$\Delta N^{a,b}_{\Delta\lambda} = N^{a}_{\Delta\lambda} - N^{b}_{\Delta\lambda} \tag{3}$$

The effect of altitude on this difference can be seen by using equation 1 to obtain the apparent spectral radiance difference:

$$\Delta N^{a,b}_{\Delta\lambda,h} = N^{a}_{\Delta\lambda,h} - N^{b}_{\Delta\lambda,h} = \left(\tau^{p}_{\Delta\lambda,h} N^{a}_{\Delta\lambda} + N^{p}_{\Delta\lambda,h}\right) - \left(\tau^{p}_{\Delta\lambda,h} N^{b}_{\Delta\lambda} + N^{p}_{\Delta\lambda,h}\right)$$

or, substituting equation 3,

$$\Delta N^{a,b}_{\Delta\lambda,h} = \tau^{p}_{\Delta\lambda,h} \Delta N^{a,b}_{\Delta\lambda} \tag{4}$$

Equation 4 predicts that the apparent radiance difference between two targets will be affected only by atmospheric transmission changes as altitude increases and will be independent of the level of path radiance, $N^{p}_{\Delta\lambda,h}$, since the latter quantity is a constant addition and cancels in the differencing. As stated previously, the path transmission will decrease with increasing altitude. Consequently, equation 4 indicates that the apparent radiance difference between two targets will also decrease with increasing altitude.

2.2.2. ATMOSPHERIC MODELS. The expected direction of the variation of apparent target radiance with altitude can be related to the manner of interaction of the radiation and the atmosphere. As stated previously, the atmosphere alters the radiation from the target by either scattering or absorption. The effects when one of these is predominant can be predicted.

2.2.2.1. Scattering Atmosphere. Suppose that the predominant manner of atmospheric interaction is scattering. The variation of apparent target radiance with altitude will depend on the magnitude of the actual target radiance relative to the average radiance of the surroundings. The surroundings include the atmosphere, clouds, the sun, and any other object from which radiation can reach the matter in the path between the target and the sensor. Three simplified conditions can hold:

(1) If the actual target radiance (per unit solid angle) is less than the average radiance of the surroundings (per unit solid angle), then the apparent target radiance must increase with altitude since the radiance from the surroundings available for scattering into the beam is greater than the target radiance available for attenuation. This is the common condition for imagery at wavelengths of less than 3 μm, where most natural targets reflect much less than 100% of the environmental radiation. This situation can also obtain for thermal wavelengths if the apparent temperature of the target is less than the average apparent temperature of the surroundings in the particular spectral band.

(2) If the actual target radiance is greater than the average radiance of the surroundings, the apparent target radiance will necessarily decrease with increasing altitude since there is not enough extraneous radiation available for scattering into the beam to make up for the actual target radiance scattered out of the beam. Such a situation usually obtains only when the target is actively emitting radiation. For thermal wavelengths, this situation is common, requiring only that the target have a higher apparent temperature than the average of the surroundings. For wavelengths at which solar radiation dominates (<3 μm), such a situation usually obtains only when a target actively emits light under low solar illumination conditions (e.g., city lights at night), or possibly when direct solar radiation is specularly reflected by a high-reflectance target.

(3) If the actual target radiance is equal to the average radiance of the surroundings, the situation is equivalent to the target being part of an integrating sphere, or "holraum." No variation in apparent radiance with altitude is to be expected since the actual target radiance attenuated by scattering is made up for exactly by the extraneous radiance scattered into the beam.

2.2.2.2. Absorbing Atmosphere. For an atmosphere which interacts with the target radiation only by absorption, the variation of apparent target radiance with altitude becomes much more straightforward than for the scattering case. For radiation at wavelengths less than about 3 μm, the only effect of the path is to attenuate and thus decrease the apparent target radiance with altitude, since for realistic atmospheric temperatures, the self emission of the path is negligible. The relationship between the target radiance and the average radiance of the surroundings is of no consequence in this case. For thermal infrared wavelengths, however, the atmospheric path can emit significant radiation, and in fact there is an equivalence between the absorptivity and emissivity of a given path. As a consequence, the relative effect of the path depends only upon the relative temperature of the path and of the target. Assuming, for simplicity, a blackbody target and uniform path temperature, if $N^{BB}(T^i)$ is the actual radiance of a blackbody at temperature T^i, then equation 1 (defining apparent radiance) can be rewritten

$$\begin{aligned} N^t_{\Delta\lambda,h} &= \tau^p_{\Delta\lambda,h} N^t_{\Delta\lambda} + N^p_{\Delta\lambda,h} \\ &= \left(1 - \alpha^p_{\Delta\lambda,h}\right) N^{BB}_{\Delta\lambda}(T^t) + \epsilon^p_{\Delta\lambda,h} N^{BB}_{\Delta\lambda}(T^p) \\ &= N^{BB}_{\Delta\lambda}(T^t) + \alpha^p_{\Delta\lambda,h}\left[N^{BB}_{\Delta\lambda}(T^p) - N^{BB}_{\Delta\lambda}(T^t)\right] \end{aligned} \qquad (5)$$

since, from Kirchhoff's law, $\alpha^p = \epsilon^p$. Thus, the apparent target radiance will be greater than, equal to, or less than the actual target radiance, depending upon whether the atmospheric path temperature, T^p, is greater than, equal to, or less than the target temperature, T^t. The degree of absorption affects only the magnitude and not the direction of this change.

2.2.2.3. Real Atmosphere. A real atmosphere will affect target radiation by simultaneous scattering and absorption. A comparison of the qualitative aspects of each indicates that, depending upon conditions, scattering and absorption can either reinforce or counteract each other in altering the apparent target radiance. It is possible, however, to make some general statements as to the relative importance of the two. In the near-ultraviolet and blue portions of the spectrum, for instance, it is known that scattering is usually predominant. This is due to the high degree of molecular (Rayleigh) scattering which varies inversely as the fourth power of the wavelength. Conversely, at infrared wavelengths, absorption is often predominant

because of the presence of numerous water-vapor and carbon-dioxide absorption bands. At intermediate wavelengths, the relative importance of scattering and absorption can be expected to be dependent upon the specific atmospheric conditions.

3
EXPERIMENTAL RESULTS

3.1. DATA USED

The data chosen for analysis were acquired during the summer of 1966 at the Agronomy Farm of Purdue University near Lafayette, Indiana. On 26 July 1966, multichannel imagery was acquired in consecutive passes at altitudes of 6000, 4000, and 2000 ft. On 15 September 1966, multichannel imagery was acquired at five altitudes ranging from 10,000 to 2000 ft. In both cases, the altitudes were flown in descending order to minimize the time lapse between the first and last passes. The data analyzed were acquired by the 12-channel spectrometer, which senses in 12 contiguous narrow bands over the wavelength range from 0.4 to 1.0 μm. Table I shows the spectral range for each of the 12 channels. These data were calibrated at the time of acquisition, so that subsequent processing in the laboratory produced apparent spectral radiance signatures for the targets of interest. The complete multichannel scanning system and the processing procedure used are described in the appendix. Absolute apparent radiances as a function of spectrometer channel and altitude were obtained for maturing soybeans and winter wheat stubble on 26 July and for mature corn and wilting soybeans on 15 September. The type of data obtained can be seen in figures 1 and 2. It should be noted that these are not true spectral representations, since each channel measures the average radiance in a relatively wide band, and the straight lines connecting individual channels have been drawn only for convenience. There are, however, recognizable spectral shapes. For example, for the maturing soybeans (fig. 1a), expected radiance peaks appear in the green (channel 8) and near-infrared (channels 11 and 12), separated by channels of reduced response which include the chlorphyll absorption region.

3.2. VARIATION IN APPARENT RADIANCE

Variations in apparent spectral radiance with altitude can be seen in figures 1 and 2, but general trends are better indicated by figures 3 and 4, which present the data in terms of normalized radiance (radiance ratio) versus altitude. The normalization is relative to the apparent spectral radiance at 2000 ft:

$$\text{Normalized Radiance} = \frac{N_{\Delta\lambda,h}}{N_{\Delta\lambda,2000}} \qquad (6)$$

TABLE I. SPECTRAL BANDWIDTHS OF THE 12-CHANNEL SPECTROMETER
(Defined for 50% response level)

Spectrometer Channel	Spectral Bandwidth (μm)
1	0.404-0.437
2	0.437-0.464
3	0.464-0.482
4	0.482-0.502
5	0.502-0.524
6	0.524-0.549
7	0.549-0.580
8	0.580-0.617
9	0.617-0.659
10	0.659-0.719
11	0.719-0.799
12	0.799-1.000

Such a ratio provides a more straightforward means of comparing the relative change with altitude in apparent radiance among the several spectral bands.

Figure 3 shows curves from the 26 July run. In general, the ratio, and thus the apparent radiance, is seen to increase with altitude in all spectral channels, with the increase being more prominent in the shorter wavelengths (lower-numbered spectrometer channels). Comparison with theory (secs. 2.2.2.1 and 2.2.2.2) indicates that, for these data, scattering and not absorption was the dominant atmospheric effect; the inverse variation of the magnitude of this phenomenon with wavelength is commensurate with the Rayleigh theory for molecular scattering.

Figure 4 shows curves from the 15 September run. Although the spectral ordering is similar to that in figure 3, there is a tendency for the radiance ratio to decrease with altitude at the longer wavelengths. It is not known if this phenomenon is real, however. The intensity of solar illumination increased considerably between the flights at 10,000 ft (0850 hours) and 2000 ft (0947 hours). An attempt was made to compensate for this illumination change at each altitude by using ground-based solar illumination measurements made at the time. The correction procedure was necessarily approximate since the ground measurements were made by a very broadband instrument, and the spectrally integrated values had to be divided theoretically into contributions from each of the 12 spectral bands represented in the spectrometer. The trends in figure 4 could be real, however, indicating that for the longer wavelengths, the atten-

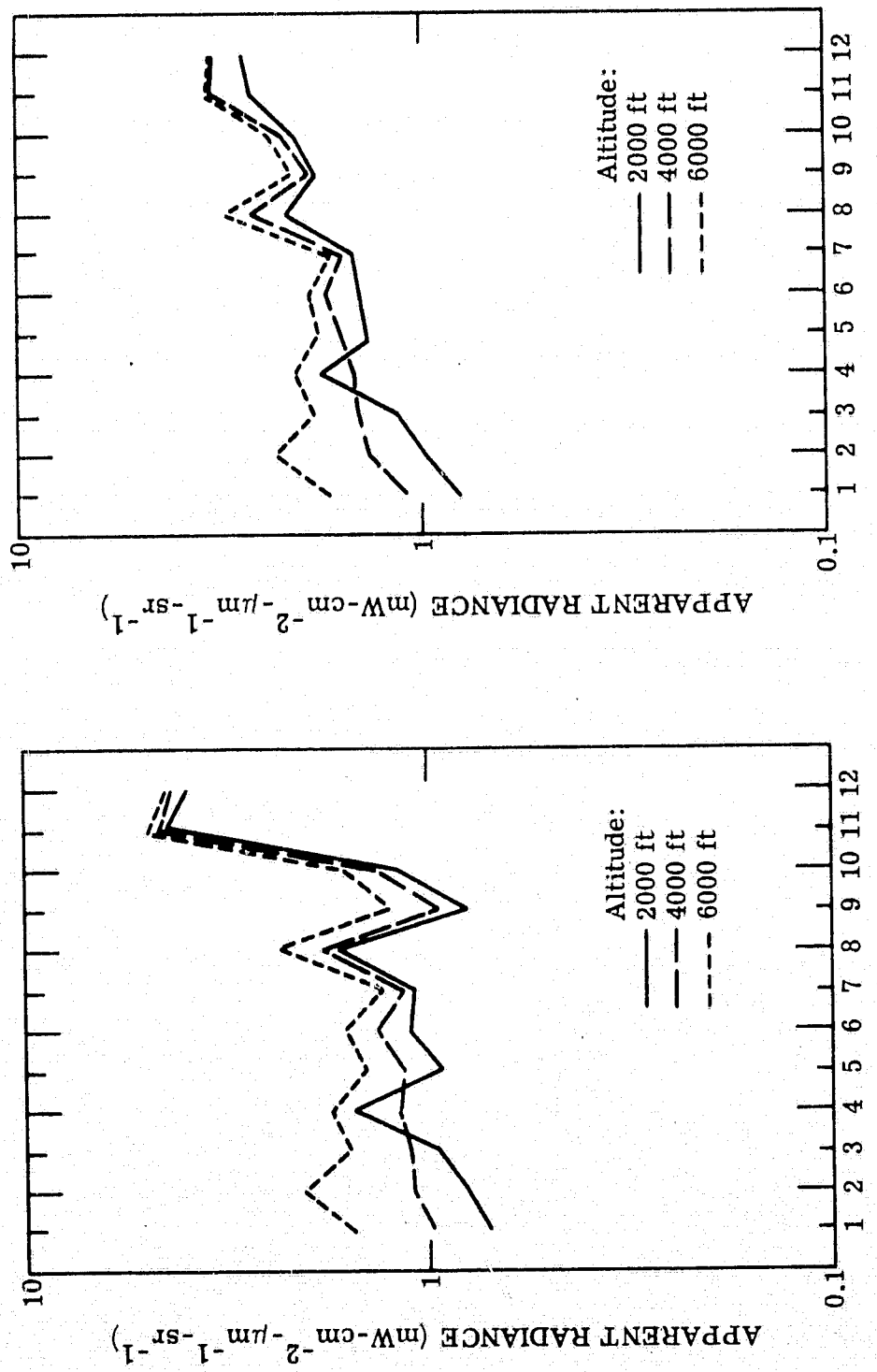

FIGURE 1. APPARENT SPECTRAL RADIANCE OF MATURING SOYBEANS AND WHEAT STUBBLE.
Data acquired 26 July 1966. Atmospheric conditions: clear with noticeable haze.

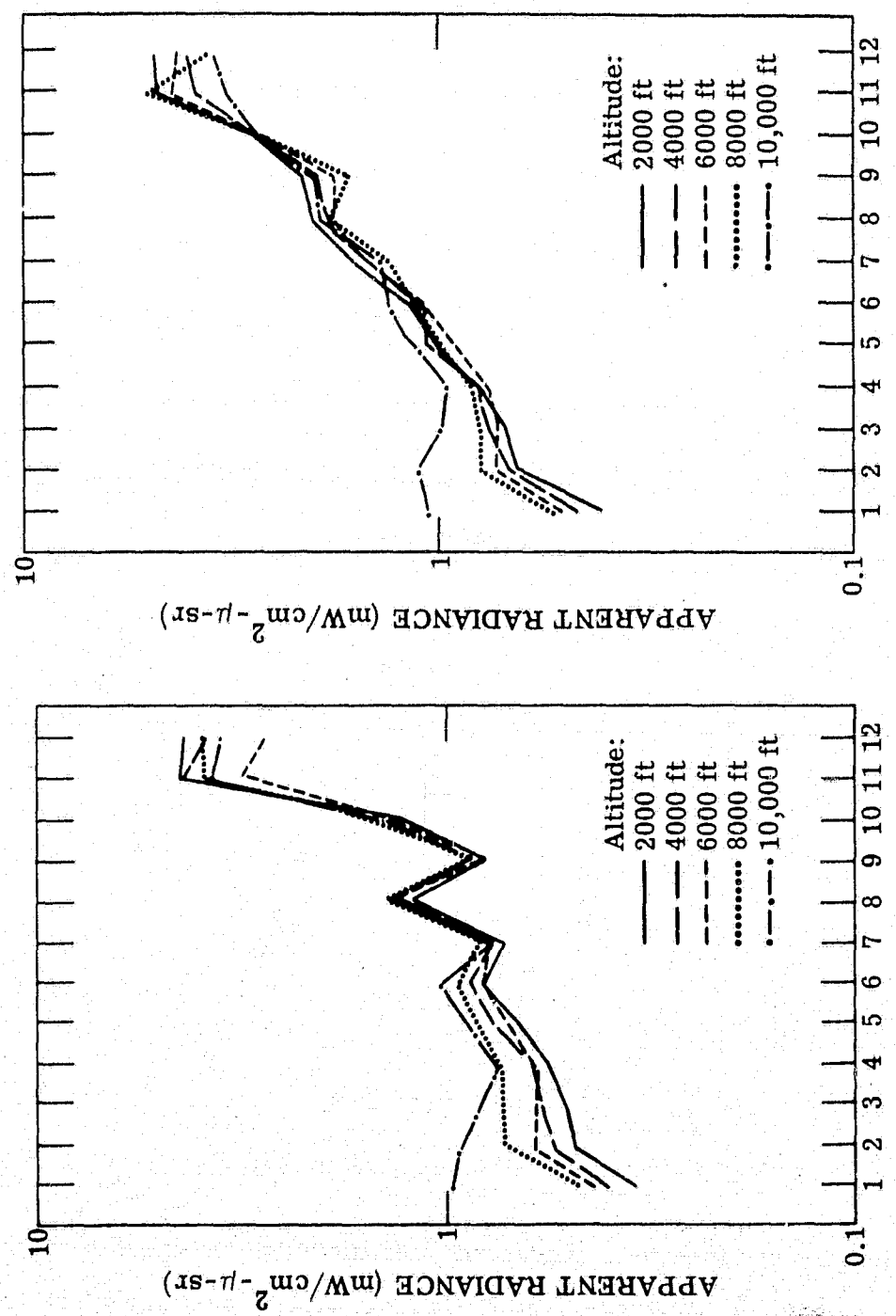

FIGURE 2. APPARENT SPECTRAL RADIANCE OF MATURE CORN AND WILTING SOYBEANS. Data acquired 15 September 1966. Atmospheric conditions: clear.

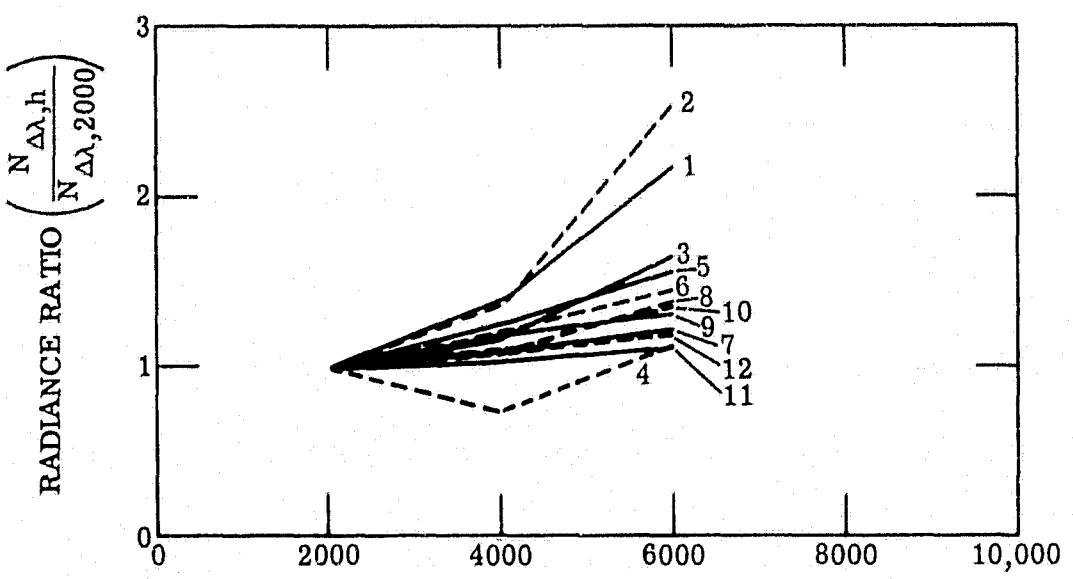

(a) Maturing Soybeans

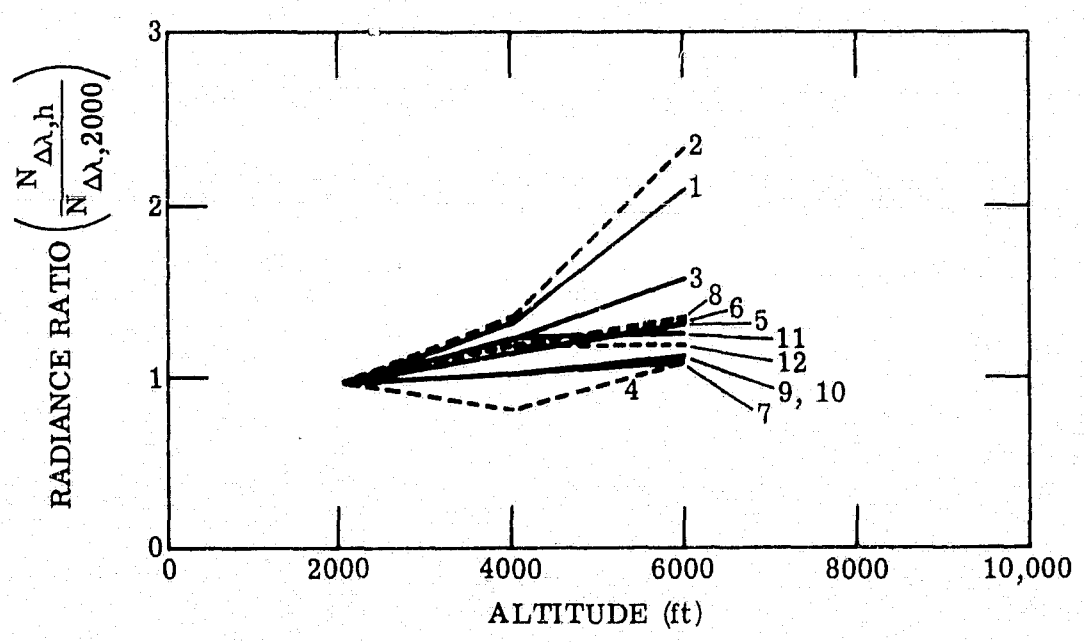

(b) Winter Wheat Stubble

FIGURE 3. RADIANCE RATIO VERSUS ALTITUDE FOR MATURING SOYBEANS AND WHEAT STUBBLE
(Parameter is spectrometer channel)

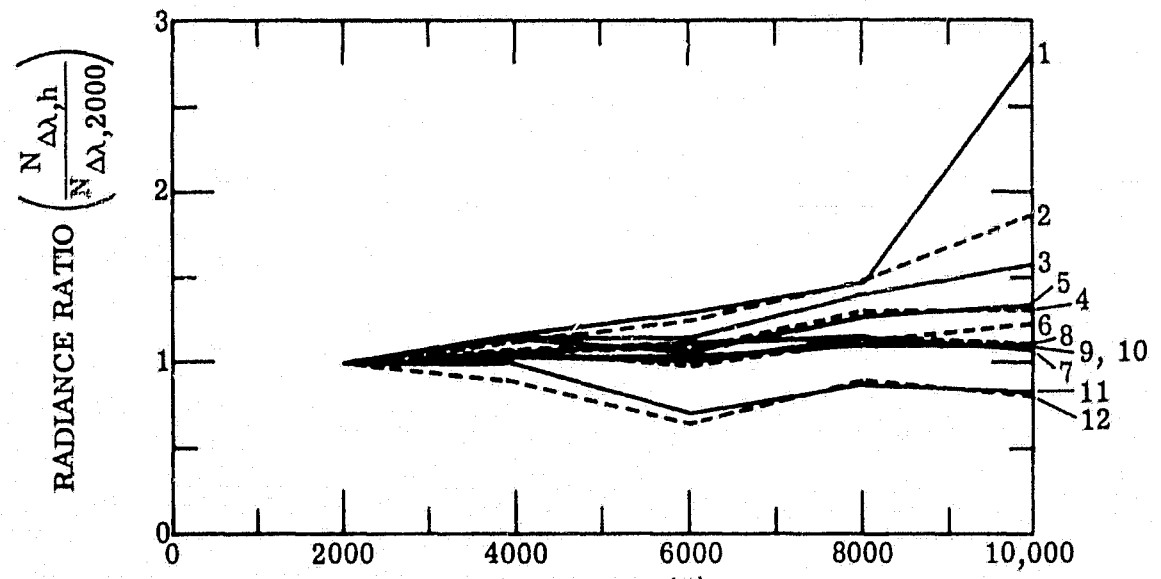

(a) Mature Corn

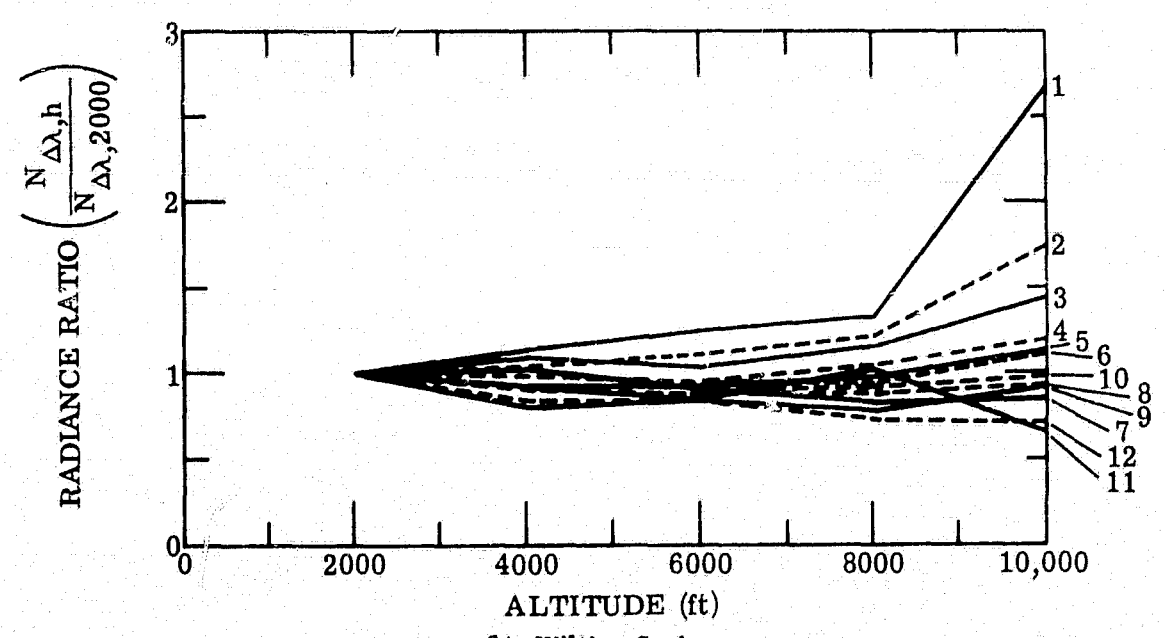

(b) Wilting Soybeans

FIGURE 4. RADIANCE RATIO VERSUS ALTITUDE FOR MATURE CORN AND WILTING SOYBEANS
(Parameter is spectrometer channel)

uation of the actual target radiance might well overcome the tendency of extraneous radiation to increase the apparent radiance with altitude. Such a condition could mean that scattering had less effect on these data than on those taken on 26 July.

The apparent differences between the results in figures 3 and 4 can probably be ascribed to the atmospheric conditions. On 26 July, the atmosphere was quite hazy, while on 15 September, it was clear with no discernible haze. Consequently, the effects of scattering would have been greater on 26 July than on 15 September, leading to an increased amount of extraneous radiation $\left(N^{p}_{\Delta\lambda,h}\right)$ in the apparent radiances and an increase in those radiances with altitude. The fact that attenuation also increases as scattering increases does not necessarily alter this conclusion (see sec. 2.2.2.1).

In section 2.2.1, it was stated that, according to theory, the direction of change with altitude of apparent radiance depends upon the magnitude of the actual target radiance in such a way that, the larger the actual target radiance, the less positive the change. This was implied in equation 2 since $\partial\tau^{p}/\partial h$ is negative. Similarly, if the radiance ratio were differentiated with respect to altitude, the same relationship would hold, since the denominator of the ratio is a constant with respect to altitude. Thus, according to theory, if for two targets, a and b,

$$N^{a}_{\Delta\lambda} > N^{b}_{\Delta\lambda} \tag{7}$$

it must follow that, for h > 2000 ft,

$$\frac{N^{a}_{\Delta\lambda,h}}{N^{a}_{\Delta\lambda,2000}} < \frac{N^{b}_{\Delta\lambda,h}}{N^{b}_{\Delta\lambda,2000}} \tag{8}$$

since the apparent radiance of target a must change less positively with increasing altitude than the apparent radiance of target b. Tables II and III summarize the results of such a comparison for the 26 July and 15 September data, respectively. In each table, the second column indicates whether the difference between the actual radiances of the crops is positive or negative, and the third column indicates whether the difference between the respective radiance ratios as presented in figures 3 and 4 is positive or negative. The general results shown in these tables are in obvious agreement with the relations in inequalities 7 and 8; i.e., the sign of the difference in actual target radiance is opposite to the sign of the difference in radiance ratio. The one exception to this is in the data for spectrometer channel 4 in table II, where the radiance ratios for soybeans and wheat stubble are identical even though the actual radiances are not. No explanation has been found for this anomaly, but it is evident from figures 1 and 3 that spectrometer channel 4 behaves quite suspiciously for the data acquired at 2000 ft on 26 July. It should be noted that table III does not contain entries for spectrometer channels 11 and

TABLE II. DIFFERENCE IN ACTUAL TARGET RADIANCE COMPARED WITH DIFFERENCE IN APPARENT RADIANCE RATIO FOR WHEAT STUBBLE AND SOYBEANS
(Data acquired 27 July 1966)

Spectrometer Channel	$N_{\Delta\lambda}^{wheat} - N_{\Delta\lambda}^{soybeans}$	$\frac{N_{\Delta\lambda,6000}^{wheat}}{N_{\Delta\lambda,2000}^{wheat}} - \frac{N_{\Delta\lambda,6000}^{soybeans}}{N_{\Delta\lambda,2000}^{soybeans}}$
1	+	-
2	+	-
3	+	-
4	+	=
5	+	-
6	+	-
7	+	-
8	+	-
9	+	-
10	+	-
11	-	+
12	-	+

TABLE III. DIFFERENCE IN ACTUAL TARGET RADIANCE COMPARED WITH DIFFERENCE IN APPARENT RADIANCE RATIO FOR CORN AND SOYBEANS
(Data acquired 15 September 1966)

Spectrometer Channel	$N_{\Delta\lambda}^{corn} - N_{\Delta\lambda}^{soybeans}$	$\frac{N_{\Delta\lambda,10,000}^{corn}}{N_{\Delta\lambda,2000}^{corn}} - \frac{N_{\Delta\lambda,10,000}^{soybeans}}{N_{\Delta\lambda,2000}^{soybeans}}$
1	-	+
2	-	+
3	-	+
4	-	+
5	-	+
6	-	+
7	-	+
8	-	+
9	-	+
10	-	+

12, because the excessive noise present in the reduction of the data for these channels precluded unambiguous determination of the sign of the difference in actual radiance between the corn and soybeans.

3.3. VARIATION IN APPARENT RADIANCE DIFFERENCE

In the foregoing discussions, the combined effect of attenuation loss and extraneous radiation gain on the apparent radiance of a target and the relative effect of the magnitude of the actual target radiance on the direction of change with altitude have been shown. The effect of attenuation alone may be studied by observing the apparent radiance difference between two targets as a function of altitude. As indicated by equation 4, the apparent radiance difference between two targets varies directly with the path transmission function, $\tau^{p}_{\Delta\lambda,h}$ and is independent of the extraneous path radiance, $N^{p}_{\Delta\lambda,h}$. Thus, theoretically, the apparent radiance difference must decrease (or at best remain constant) with altitude, since the atmospheric transmission function must decrease (or remain constant) as the path length increases. Figures 5 and 6 show the apparent spectral radiance differences, as a function of altitude, for the crops scanned on 26 July and 15 September, respectively.

For figure 5, passes were made at 2000, 4000, and 6000 ft. It is difficult to define any trend in these curves. For some spectrometer channels, the radiance difference decreases slightly with altitude, for some it appears to increase slightly, and for still others it varies ambiguously. Such results, when compared with theory, indicate that for the hazy conditions that obtained on 26 July, any change in $\tau^{p}_{\Delta\lambda,h}$ between 2000 and 6000 ft was insignificant considering the uncertainties in the data caused by system noise, sampling techniques, or the possible slight differences in illumination at the three altitudes.

In figure 6 (ignoring for the moment the data acquired at 10,000 ft), the variation with altitude appears to be systematic. In general, the apparent radiance difference decreases with altitude to such an extent that at 8,000 ft, the apparent difference $\left(\text{and thus } \tau^{p}_{\Delta\lambda,h}\right)$ is only one-half the value at 2,000 ft. Such a significant variation of $\tau^{p}_{\Delta\lambda,h}$ with altitude for the clear conditions on 15 September seems rather odd when no such variation was noted for the hazy conditions on 26 July (fig. 5), under which variation would be more likely to occur. As discussed earlier, this apparent effect might be due to some systematic error involved in accounting for the significant illumination changes known to have taken place during the flights on 15 September. The nonsystematic behavior of the data from the pass at 10,000 ft may also be due to such error. In any case, it is felt that the data in figure 5 were less subject to uncertainties and systematic errors and thus are probably more indicative of the real variation of $\tau^{p}_{\Delta\lambda,h}$ with altitude than the data in figure 6.

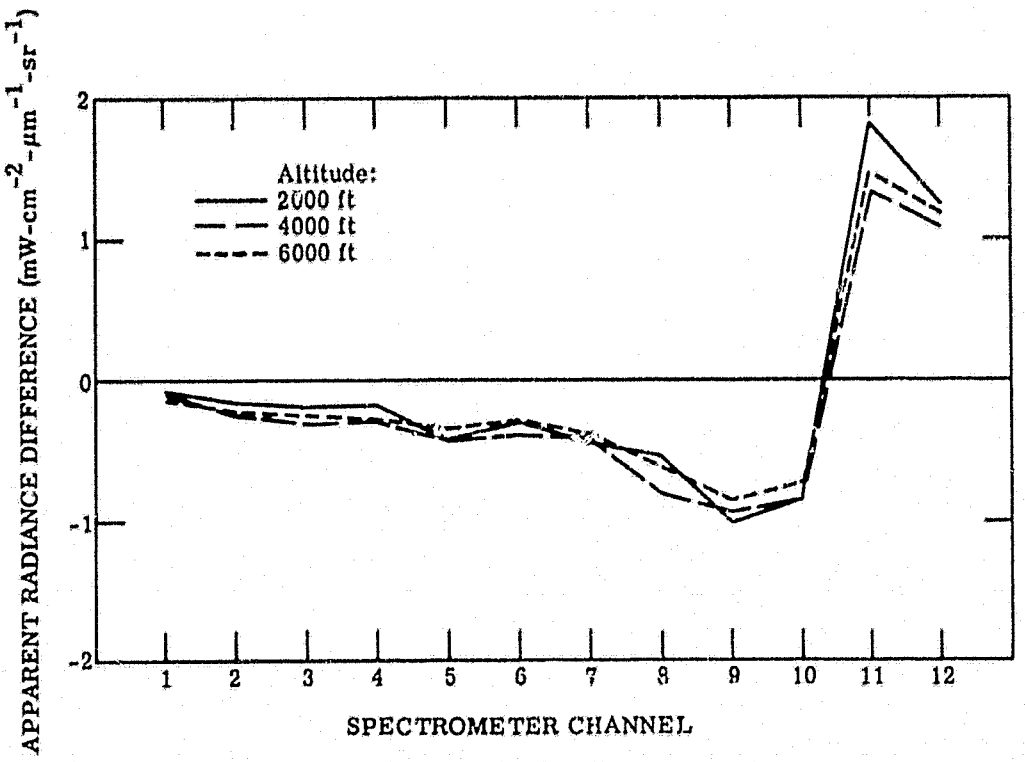

FIGURE 5. APPARENT SPECTRAL RADIANCE DIFFERENCE BETWEEN MATURING SOYBEANS AND WHEAT STUBBLE

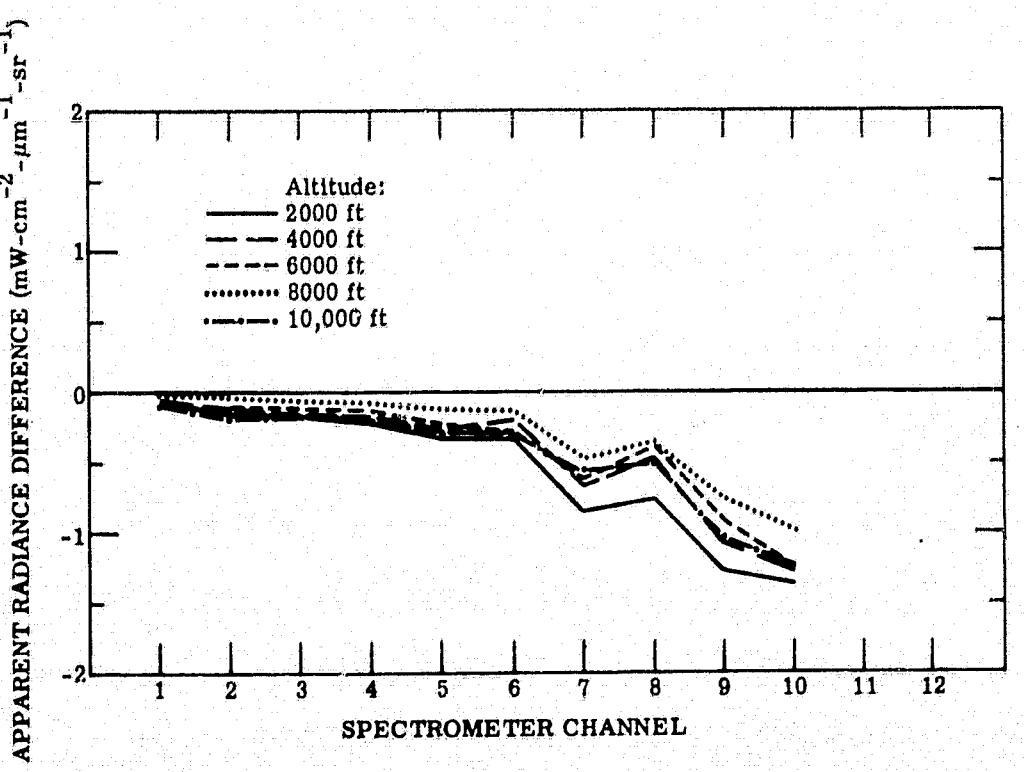

FIGURE 6. APPARENT SPECTRAL RADIANCE DIFFERENCE BETWEEN MATURE CORN AND WILTING SOYBEANS

4 DISCUSSION OF THE RESULTS

We have seen how the apparent spectral radiance of a target can vary as a function of altitude. We now consider the effects of such variation on the operation of airborne remote sensor systems.

4.1. EFFECTS OF ALTITUDE ON THE OPERATION OF SCANNERS

4.1.1. SIGNAL VARIATION. Optical-mechanical scanners use detectors which transform the radiation signal into a voltage. A simplified representation of this process would be as follows:

$$V^{t}_{\Delta\lambda,h} = R_{\Delta\lambda} N^{t}_{\Delta\lambda,h} + V^{o}_{\Delta\lambda} \tag{9}$$

where $V^{t}_{\Delta\lambda,h}$ = recorded voltage from system at altitude h looking at target t in spectral channel $\Delta\lambda$

$R_{\Delta\lambda}$ = responsivity of system

$N^{t}_{\Delta\lambda,h}$ = apparent radiance of target

$V^{o}_{\Delta\lambda}$ = arbitrary dc voltage applied for recording purposes

Using equation 1, equation 9 may be expanded to

$$\begin{aligned} V^{t}_{\Delta\lambda,h} &= R_{\Delta\lambda}\left(\tau^{p}_{\Delta\lambda,h} N^{t}_{\Delta\lambda} + N^{p}_{\Delta\lambda,h}\right) + V^{o}_{\Delta\lambda} \\ &= R_{\Delta\lambda}\tau^{p}_{\Delta\lambda,h} N^{t}_{\Delta\lambda} + R_{\Delta\lambda} N^{p}_{\Delta\lambda,h} + V^{o}_{\Delta\lambda} \end{aligned} \tag{10}$$

From equation 10, it follows that, since $R_{\Delta\lambda}$ and $V^{o}_{\Delta\lambda}$ can be arbitrarily selected by changing the gain and dc offset of the system, respectively, it is possible to negate any change in the path transmission coefficient, $\tau^{p}_{\Delta\lambda,h}$, by changing $R_{\Delta\lambda}$ and to eliminate altogether the extraneous path radiance by choosing $V^{o}_{\Delta\lambda} = -R_{\Delta\lambda} N^{p}_{\Delta\lambda,h}$. As a consequence, then, it would seem that an optical-mechanical scanner system could compensate for any effects of altitude on signal strength, thus maintaining the signal output within the optimum dynamic range for recording.

4.1.2. SIGNAL-TO-NOISE VARIATION. In practice, optimum utilization of the above characteristics of the scanner system is ultimately limited by noise considerations. The signal-to-noise ratio (SNR) of the recorded information can be reduced as the effects of the atmospheric path on the target radiance increase. For the purpose of this discussion, let the

information in which we are interested be the recorded voltage difference between two targets, a and b, between which we wish to discriminate. The SNR can then be defined as

$$SNR = \frac{V^a_{\Delta\lambda,h} - V^b_{\Delta\lambda,h}}{\Delta V^n} = \frac{R_{\Delta\lambda}\tau^p_{\Delta\lambda,h}\Delta N^{a,b}_{\Delta\lambda}}{\Delta V^n} \tag{11}$$

where $V^a_{\Delta\lambda,h}$ and $V^b_{\Delta\lambda,h}$ are as defined above, ΔV^n is the noise voltage, and $\Delta N^{a,b}_{\Delta\lambda}$ is the actual radiance difference between a and b as defined by equation 3. The operational implications of equation 11 depend upon the limiting-noise source producing ΔV^n. Three general conditions can obtain background-noise limiting, detector-noise limiting, and system-noise limiting.

4.1.2.1. Background-Noise Limiting. A background-noise-limited system is theoretically the optimum system. The limiting noise is produced by the intrinsic statistical fluctuation in arrival rate of photons at the detector from the background. The background is composed of the atmosphere, spectral filter, window material, mirrors, and other objects besides the target in the instantaneous field of view. According to classical statistics, the mean-square fluctuation in the number of photons is proportional to the average number of photons. Thus, the rms noise-equivalent radiance variation is proportional to the square root of the average radiance, and the SNR relation of equation 11 becomes

$$SNR = \frac{R_{\Delta\lambda}\tau^p_{\Delta\lambda,h}\Delta N^{a,b}_{\Delta\lambda}}{R_{\Delta\lambda}k(\overline{N}_{\Delta\lambda,h})^{1/2}} = \frac{\tau^p_{\Delta\lambda,h}\Delta N^{a,b}_{\Delta\lambda}}{k(\overline{N}_{\Delta\lambda,h})^{1/2}} \tag{12}$$

where $\overline{N}_{\Delta\lambda,h}$ is the average radiance on the detector, and k is a constant. Thus, not only will the decrease in $\tau^p_{\Delta\lambda,h}$ with altitude decrease the SNR, but also any increase in apparent target radiance will further decrease the SNR. Equation 12 should not be construed to imply that a decrease with altitude in apparent target radiance will increase the SNR, since any decrease in $\overline{N}_{\Delta\lambda,h}$ must be caused by a decrease in $\tau^p_{\Delta\lambda,h}$. The best possible condition would be when $\overline{N}_{\Delta\lambda,h}$ decreases proportionally with $\tau^p_{\Delta\lambda,h}$, at which time the SNR would still decrease at a rate proportional to $\left(\tau^p_{\Delta\lambda,h}\right)^{1/2}$.

4.1.2.2. Detector-Noise Limiting. A detector can introduce noise into the signal in several ways, depending upon the type of detector and its operating conditions. In general, the magnitude of the noise is stated in terms of an equivalent fluctuation in energy incident upon the detector. Consequently, the SNR relation of equation 11 for a detector-noise-limited system becomes

$$SNR = \frac{R_{\Delta\lambda}\tau^{p}_{\Delta\lambda,h}\Delta N^{a,b}_{\Delta\lambda}}{R_{\Delta\lambda}\Delta N^{n}} = \frac{\tau^{p}_{\Delta\lambda,h}\Delta N^{a,b}_{\Delta\lambda}}{\Delta N^{n}} \tag{13}$$

where ΔN^{n} is the constant noise-equivalent radiance fluctuation at the detector. Thus, the variation with altitude of the SNR depends only upon the atmospheric attenuation (not upon the magnitude of the average radiance, as with the background-noise-limited condition). However, even though this indicates that the SNR for a detector-noise-limited system can, for some conditions, vary less with altitude than a background-noise-limited system, it must be noted that the SNR for the former is inherently lower and remains lower.

4.1.2.3. System-Noise Limiting. In general terms, system noise is any noise entering the signal from the detector output through the recording medium. It takes the form of a noise voltage of some magnitude at the output of the component which produces it. In order to characterize the effect of such noise, it is useful to define the responsivity, $R_{\Delta\lambda}$, of the system in the following manner:

$$R_{\Delta\lambda} = R^{d}_{\Delta\lambda}G_1G_2 \cdots G_r = R^{d}_{\Delta\lambda}\prod_{i=1}^{r} G_i \tag{14}$$

where $R^{d}_{\Delta\lambda}$ is the responsivity of the detector-optics combination, and G_i is the gain of the ith component of the system. Now the noise introduced by the ith component is commonly defined as the product of G_i and an equivalent noise voltage at the input to that component, ΔV^{n}_{i}. Thus, the total noise voltage at the system output is

$$\Delta V^{n} = \Delta V^{n}_{1}G_1G_2 \cdots G_r + \Delta V^{h}_{2}G_2G_3 \cdots G_r + \cdots + \Delta V^{n}_{r-1}G_{r-1} + \Delta V^{n}_{r}G_r = \sum_{j=1}^{r}\left(\Delta V^{n}_{j}\prod_{i=j}^{r} G_i\right) \tag{15}$$

Using equation 11, the SNR for the system is

$$SNR = \frac{R_{\Delta\lambda}\tau^{p}_{\Delta\lambda,h}\Delta N^{a,b}_{\Delta\lambda}}{\Delta V^{n}} = \frac{\left(R^{d}_{\Delta\lambda}\tau^{p}_{\Delta\lambda,h}\Delta N^{a,b}_{\Delta\lambda}\right)\prod_{i=1}^{r} G_i}{\sum_{j=1}^{r}\left(\Delta V^{n}_{j}\prod_{i=j}^{r} G_i\right)} \tag{16}$$

As with the detector-noise-limited condition, the SNR, when system-noise limited, will depend directly upon variations in $\tau^{p}_{\Delta\lambda,h}$ but will be independent of variations in total apparent radiance

caused by atmospheric path effects. Unlike the previous cases, however, equation 16 indicates that it might be possible to counteract the effect of $\tau^{p}_{\Delta\lambda,h}$ variations on SNR by changing the gain of various components, based upon the relative magnitudes of the individual noise voltages. (Indeed, it appears possible to actually increase the SNR with altitude even as $\tau^{p}_{\Delta\lambda,h}$ decreases. In fact, however, this is of no practical interest because it is possible only if the SNR is degraded at the lower altitudes.) In any event, the SNR for the system-noise-limited condition is inherently lower than for the other conditions.

4.2. EFFECTS OF ALTITUDE ON THE OPERATION OF PHOTOGRAPHIC SYSTEMS

4.2.1. SIGNAL VARIATION. Cameras use radiation-sensitive films as detectors which transform the apparent spectral radiance of a target into a distribution of opaque silver grains on a base material. The normal measure of intensity for such a system is the optical density of the exposed film. For that portion of the film's dynamic range in which the density is a linear function of the logarithm of the exposure,

$$D^{t}_{\Delta\lambda,h} = \gamma_{\Delta\lambda} \log R'_{\Delta\lambda} N^{t}_{\Delta\lambda,h} + \log E^{o}_{\Delta\lambda} = \gamma_{\Delta\lambda} \log \frac{R'_{\Delta\lambda} N^{t}_{\Delta\lambda,h}}{E'_{\Delta\lambda}} \tag{17}$$

where $D^{t}_{\Delta\lambda,h}$ = recorded optical density from the system at altitude h looking at target t in spectral channel $\Delta\lambda$

$R'_{\Delta\lambda}$ = responsivity of the system, relating radiance to exposure (includes f number and shutter speed)

$N^{t}_{\Delta\lambda,h}$ = apparent radiance of target

$E^{o}_{\Delta\lambda} = (E'_{\Delta\lambda})^{\gamma}$ = intercept of the linear portion of the film curve with the exposure axis (dependent upon film type and development conditions)

$\gamma_{\Delta\lambda}$ = slope of linear D versus log E curve (dependent upon film type and development conditions)

Using the relation in equation 1, equation 17 may be expanded to

$$D^{t}_{\Delta\lambda,h} = \gamma_{\Delta\lambda} \log \frac{R'_{\Delta\lambda}\left(\tau^{p}_{\Delta\lambda,h} N^{t}_{\Delta\lambda} + N^{p}_{\Delta\lambda,h}\right)}{E'_{\Delta\lambda}} \tag{18}$$

Because of the logarithmic response of the photographic emulsion, equation 18 is quite different from equation 10, which describes the signal from an optical-mechanical scanner. Although variations in apparent radiance with altitude for a specific target can be compensated for by changes in $R'_{\Delta\lambda}$ or $\gamma_{\Delta\lambda}$, for example, this is not nearly so easy as the analogous operation

with an electrical scanner signal because of the difficulty in monitoring $D^t_{\Delta\lambda,h}$ directly. In addition, for a camera, there is no dc offset which can be used to compensate directly for $N^p_{\Delta\lambda,h}$, as can be done with the dc voltage offset, $V^o_{\Delta\lambda}$, for a scanner. Consequently, the operational constraints imposed upon a camera are somewhat more restrictive than those imposed upon a scanner with signals in electrical form.

4.2.2. SIGNAL-TO-NOISE VARIATION. As indicated earlier, the ability to compensate for the effects of variable atmospheric path on apparent target radiance is limited by noise considerations. For a photographic system, the SNR for discriminating between two targets, a and b, can be defined as

$$SNR = \frac{D^a_{\Delta\lambda,h} - D^b_{\Delta\lambda,h}}{\Delta D^n} \tag{19}$$

where $D^a_{\Delta\lambda,h}$ and $D^b_{\Delta\lambda,h}$ are the recorded densities of targets a and b as defined by equation 18, and ΔD^n is the noise-density variation. From a theoretical viewpoint, it is possible to define the same noise conditions for a camera system as for an optical-mechanical scanner system. As a practical matter, however, especially in view of the envelope of operating conditions for aerial cameras, the only noise condition with which we need be concerned is detector (film)-noise limiting.

The noise associated with a photographic emulsion (often called "grain noise," or "granularity") is due to the fact that the apparently homogeneous emulsion is really composed of discrete silver grains with generally random distribution. It can be shown* that the rms noise level in a density measurement is proportional to the square root of the density:

$$\Delta D^n = k' D^{1/2} \tag{20}$$

where the proportionality constant k' depends upon film type, development procedure, and the area over which a particular measurement of density integrates. Using the definition of density in equation 17, equation 20 becomes

$$\Delta D^n = k' \left(\gamma_{\Delta\lambda} \log \frac{R'_{\Delta\lambda} \overline{N}_{\Delta\lambda,h}}{E'_{\Delta\lambda}} \right)^{1/2} \tag{21}$$

where $\overline{N}_{\Delta\lambda,h}$ is the average radiance used to expose a particular portion of the film. Substituting equation 21 into the SNR relation of equation 19 and expanding and combining the density terms in the numerator leads to

*G. C. Higgins and K. F. Stulte, "Experimental Study of rms Granularity as a Function of Scanning Spot Size," J. Opt. Soc. Am., Vol. 49, No. 9, 1959, pp. 925-929.

$$SNR = \frac{\gamma_{\Delta\lambda} \log \dfrac{\tau^{p}_{\Delta\lambda,h} N^{a}_{\Delta\lambda} + N^{p}_{\Delta\lambda,h}}{\tau^{p}_{\Delta\lambda,h} N^{b}_{\Delta\lambda} + N^{p}_{\Delta\lambda,h}}}{k' \left(\gamma_{\Delta\lambda} \log \dfrac{R'_{\Delta\lambda} \overline{N}_{\Delta\lambda,h}}{E'_{\Delta\lambda}} \right)^{1/2}} \tag{22}$$

Equation 22 may be simplified somewhat by assuming that the apparent radiance difference between targets a and b is small compared to their average value (the case in which noise considerations are most significant). A binomial expansion of the terms in the logarithm of the numerator of equation 22 then leads to

$$SNR = \frac{\gamma_{\Delta\lambda} \log \left(1 + \dfrac{\tau^{p}_{\Delta\lambda,h} \Delta N^{a,b}_{\Delta\lambda,h}}{2\overline{N}_{\Delta\lambda,h}} \right)^{2}}{k' \left(\gamma_{\Delta\lambda} \log \dfrac{R'_{\Delta\lambda} \overline{N}_{\Delta\lambda,h}}{E'_{\Delta\lambda}} \right)^{1/2}} \tag{23}$$

Comparison of equations 23 and 13 indicates that there is a distinct qualitative difference in detector noise limitation between photographic and electronic systems. In an electronic system, the SNR decreases only as atmospheric transmission $\left(\tau^{p}_{\Delta\lambda,h}\right)$ decreases; in a photographic system, the SNR also decreases because of atmospheric radiance $\left(N^{p}_{\Delta\lambda,h}\right)$ effects, which tend to increase $\overline{N}_{\Delta\lambda,h}$. As indicated in section 4.2.1, $R'_{\Delta\lambda}$ can be varied to accommodate changes in $\overline{N}_{\Delta\lambda,h}$ and maintain the signals in the same density range on the film. This would indeed keep the denominator of equation 23 constant but would not compensate for any decrease of the numerator due to an increase in $\overline{N}_{\Delta\lambda,h}$. If $R'_{\Delta\lambda}$ is reduced even further, it appears that it can in fact compensate completely for atmospheric effects on the SNR. However, large reductions in $R'_{\Delta\lambda}$ will tend to decrease the dynamic range of the recorded data, since lower-level signals will be forced onto the nonlinear portion of the film-response curve and become lost in the fog level of the film. In any event, even though the SNR for a photographic system may degrade relatively faster with increasing altitude than the SNR for a scanner system, it must be remembered that which of these systems gives the higher absolute SNR depends upon the particular characteristics of each and upon the conditions of data acquisition.

4.3. EXAMPLES OF IMAGERY

As indicated in section 4.1.1, changes in apparent target radiance with varying atmospheric path can be compensated for quite easily in an optical-mechanical scanner because of the electrical form of the signals. This is illustrated by the imagery in figures 7a-f, taken at five different altitudes for four of the spectrometer channels and for the 0.32- to 0.38-μm ultraviolet

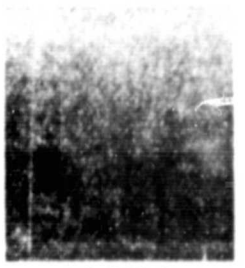

10,000 ft

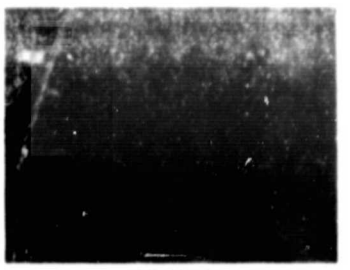

8000 ft

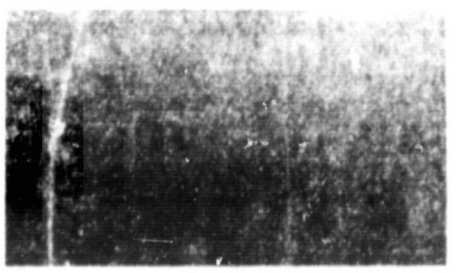

6000 ft

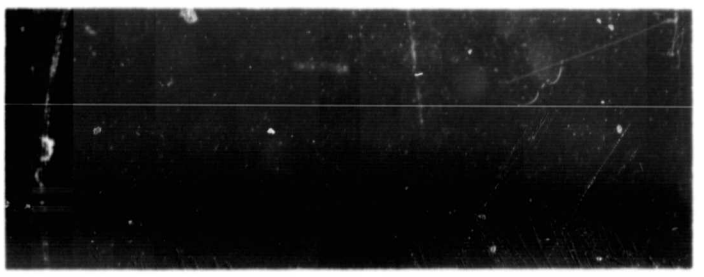

4000 ft

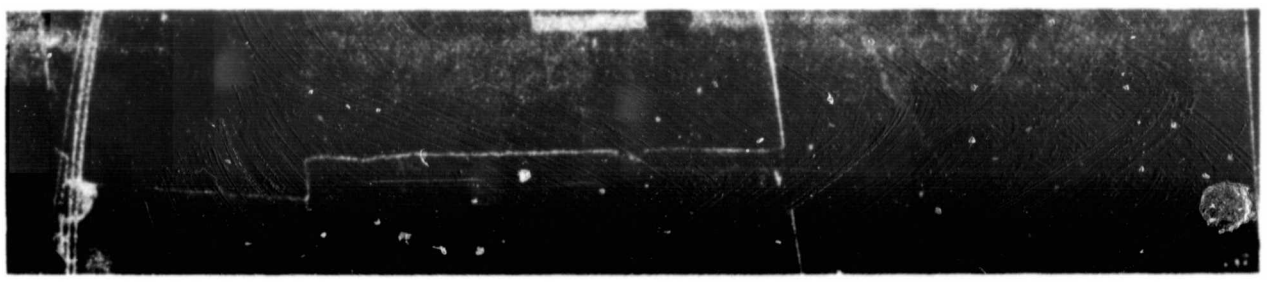

2000 ft

FIGURE 7. COMPARISONS OF SCANNER IMAGERY FOR VARIOUS WAVELENGTHS TAKEN AT SEVERAL ALTITUDES. Data acquired 15 September 1966 between 0850 and 0947 hours near the Purdue University Agronomy Farm. (a) 0.32-0.38 μm.

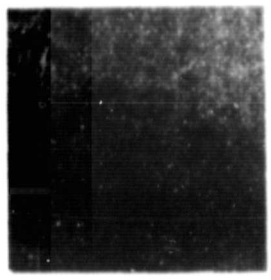

10,000 ft

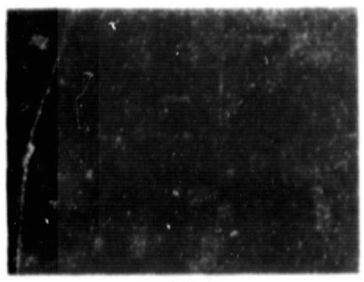

8000 ft

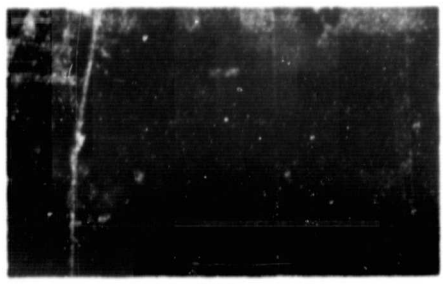

6000 ft

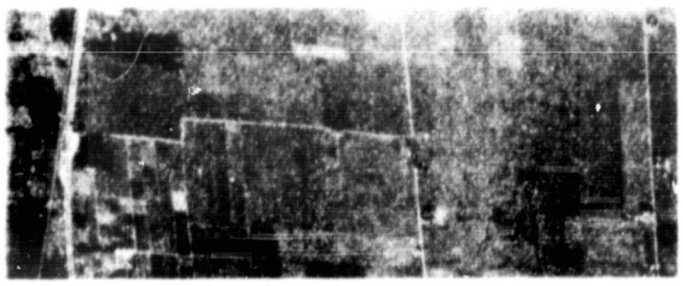

4000 ft

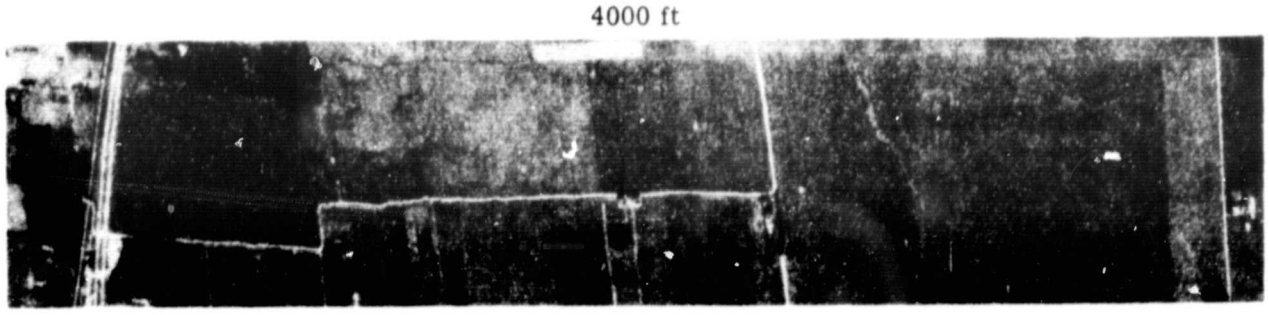

2000 ft

FIGURE 7. COMPARISONS OF SCANNER IMAGERY FOR VARIOUS WAVELENGTHS TAKEN AT SEVERAL ALTITUDES (Continued). (b) 0.404-0.437 μm, Channel 1.

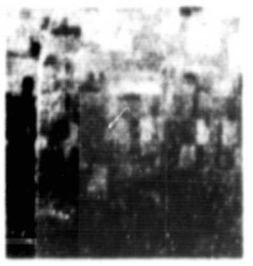

10,000 ft

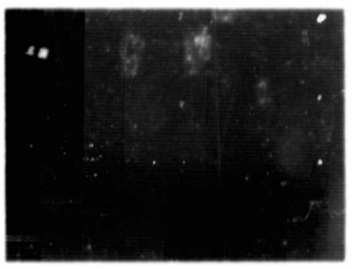

8000 ft

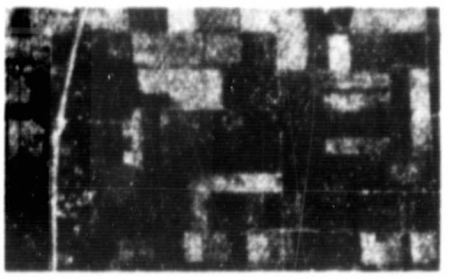

6000 ft

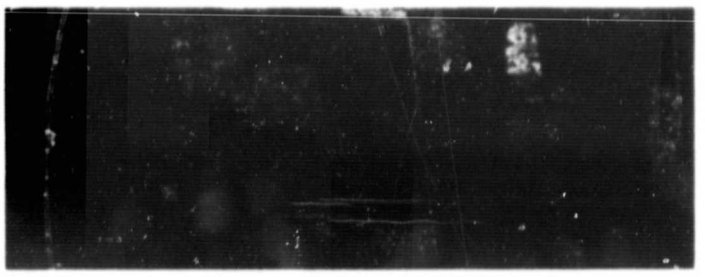

4000 ft

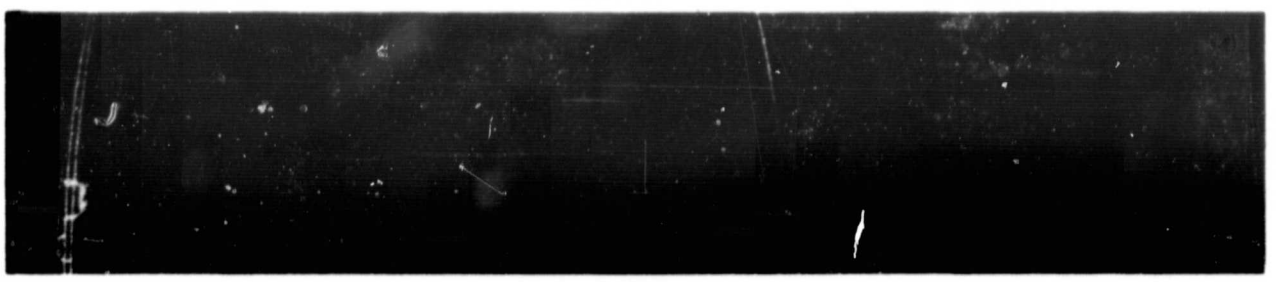

2000 ft

FIGURE 7. COMPARISONS OF SCANNER IMAGERY FOR VARIOUS WAVELENGTHS TAKEN AT SEVERAL ALTITUDES (Continued). (c) 0.549-0.580 μm, Channel 7.

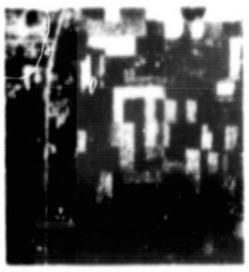

10,000 ft

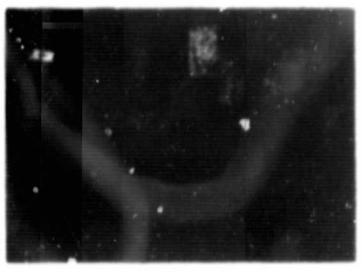

8000 ft

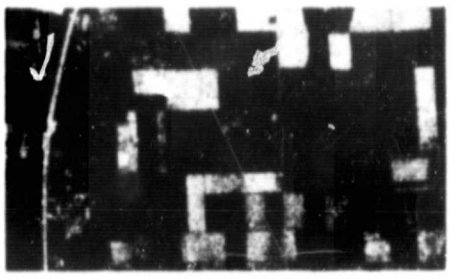

6000 ft

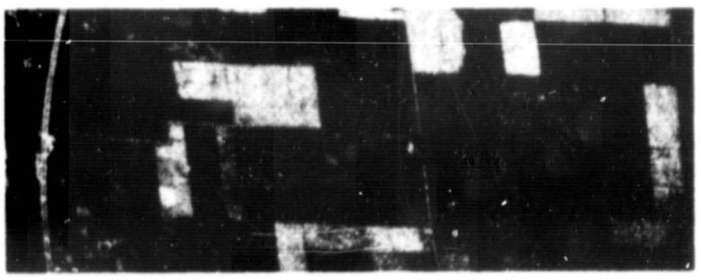

4000 ft

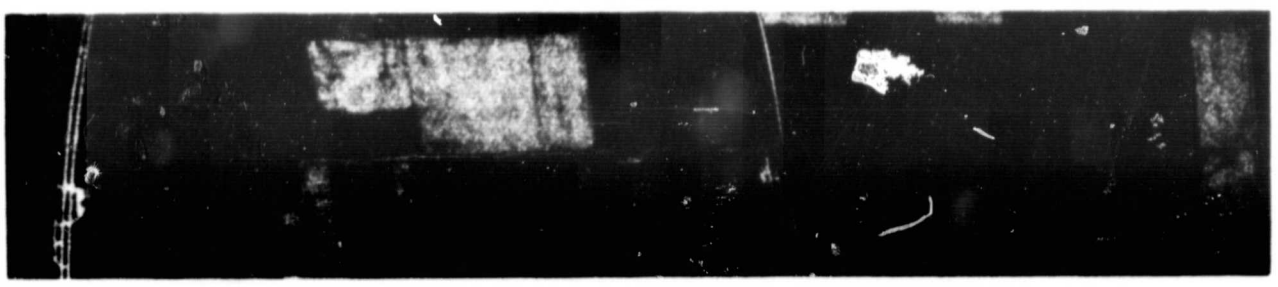

2000 ft

FIGURE 7. COMPARISONS OF SCANNER IMAGERY FOR VARIOUS WAVELENGTHS TAKEN AT SEVERAL ALTITUDES (Continued). (d) 0.617-0.659 μm, Channel 9.

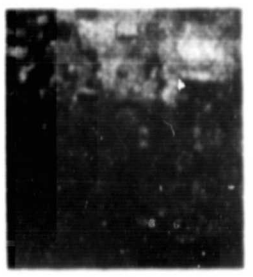

10,000 ft

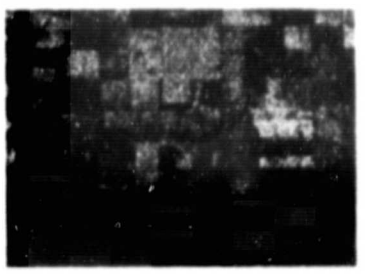

8000 ft

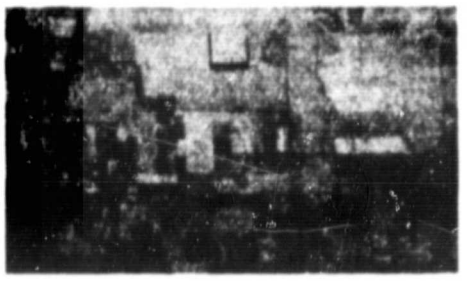

6000 ft

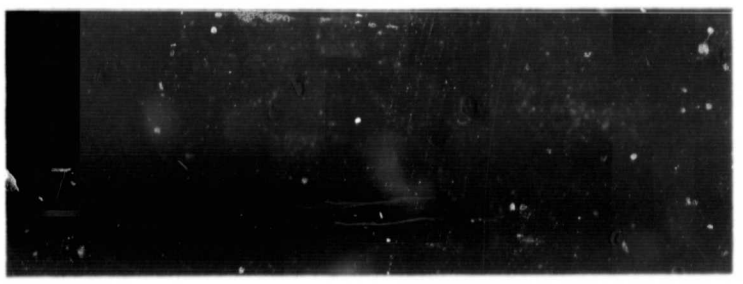

4000 ft

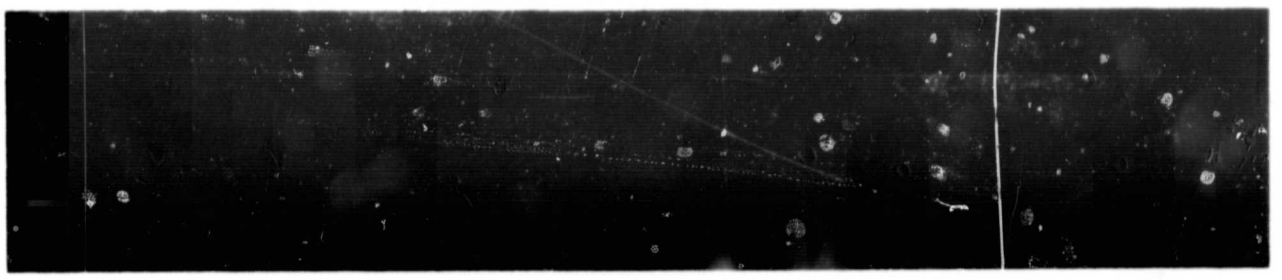

2000 ft

FIGURE 7. COMPARISONS OF SCANNER IMAGERY FOR VARIOUS WAVELENGTHS TAKEN AT SEVERAL ALTITUDES (Continued). (e) 0.799-1.0 μm, Channel 12.

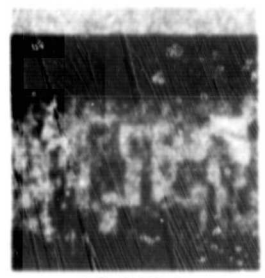

10,000 ft

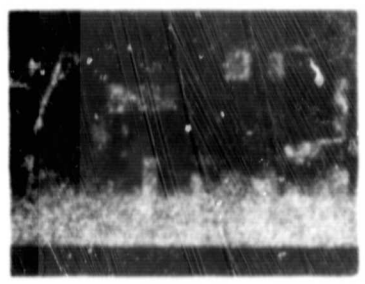

8000 ft

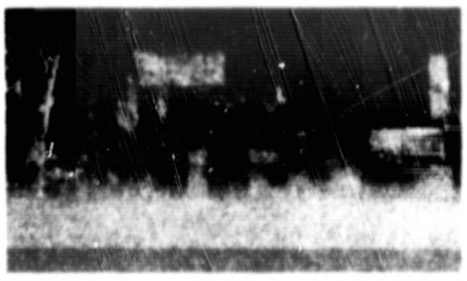

6000 ft

4000 ft

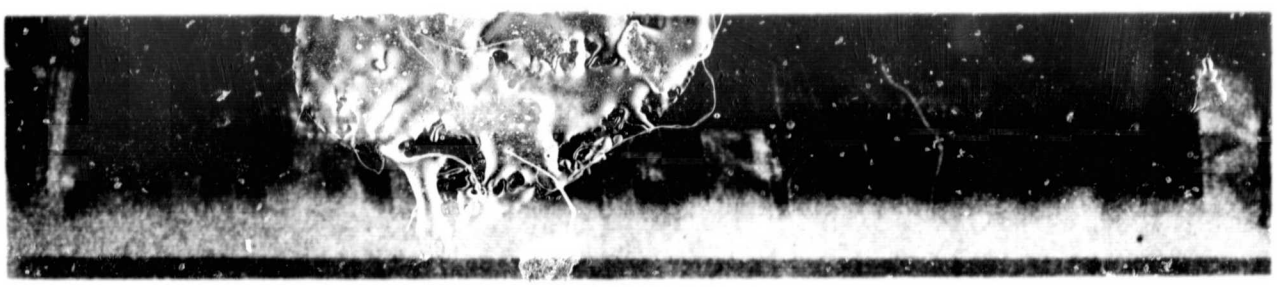

2000 ft

FIGURE 7. COMPARISONS OF SCANNER IMAGERY FOR VARIOUS WAVELENGTHS TAKEN AT SEVERAL ALTITUDES (Concluded). (f) 8.0-13.5 μm.

and 8.0- to 13.5-μm thermal infrared regions. Note that the general quality of the imagery in regard to contrast does not vary significantly with altitude, nor is there any apparent level shift due to increasing path radiance. Even in the ultraviolet (fig. 7a), where atmospheric scattering effects are extreme, little contrast is lost on account of increasing altitude except for some of the roads whose responses are diminished because of spatial-resolution limitations. Generally the upper portions of the shorter-wavelength images appear brighter than the lower portions. This is not an atmospheric effect; rather it is due to the fairly low sun elevation which produced back-scattered light from the terrain in the upper portions and forward-scattered light from the terrain in the lower portions. For agricultural targets, back-scattering reflectance is normally higher than forward-scattering reflectance. In the 8.0- to 13.5-μm imagery of figure 7f, the apparent tonal gradations at the top and bottom of each image are due to vignetting of the field of view caused by the calibration plates (see the app.).

The experimental results presented in section 3 indicate that atmospheric effects should not significantly alter spectral differences between targets. Figure 8 shows multispectral imagery of the same agricultural area taken at an altitude of 2000 ft, and figure 9 shows imagery of this area taken at 8000 ft. Comparison of figures 8 and 9 shows that spectral characteristics are not altered by a change in altitude; except for scale, the features of the imagery are identical. Note, for example, the spectral variation of field A compared to fields B and C in both figures. The subtle spectral differences at intermediate wavelengths are maintained just as truly at both altitudes as are the gross differences at the shorter and longer wavelengths.

5
CONCLUSIONS AND RECOMMENDATIONS

The results of the preliminary study in the 0.4- to 1.0-μm spectral region indicate that variations in sensor altitude and acquisition conditions can significantly alter the apparent spectral radiance of a given target. The following conclusions are indicated:

(1) An increase in sensor altitude can either increase of decrease apparent target radiance.

(2) The tendency toward increase in apparent radiance is inversely related to wavelength.

(3) The tendency toward increase in apparent radiance is significantly strengthened by hazy atmospheric conditions.

(4) The greater the actual target radiance, the less the tendency toward increase in apparent radiance with altitude.

(5) The attenuation of spectral radiance differences between objects with variation in altitude may not be significant.

(6) The decrease with altitude in recorded signal difference between two targets will tend to be greater and less easily compensated for in a photographic system than in a scanner system.

(7) The decrease with altitude of the signal-to-noise ratio will in general be greater for a photographic system than for a scanner system.

(8) Depending upon conditions, instrumentation, and type of information desired, a specific photographic system may be better than a specific scanner system in absolute terms, even though the relative atmospheric effects are greater for the photographic system.

In general, these results agree quite well with qualitative predictions based on theory. Theory cannot, however, be expected to produce much quantitative information for use in interpretation of the data. The extreme complexity of molecular absorption and emission spectra and the equally great complexity of scattering theory make such an approach impracticable. In addition, it would be quite difficult either to measure or to predict the quantities upon which a theoretical approach would depend, such as the total amount of water vapor in the path or the size and distribution of particulate matter. A continued empirical approach to the problem would be in order. This could be accomplished in two ways. First, comprehensive experiments such as those described in this report could produce a large quantity of data defining the quantitative effect of altitude variation as a function of various measurable or observable conditions. Such data could then be used to correct future remote-sensor data. Second, the remote-sensor data could be used to "bootstrap" its own altitude corrections. This would be possible if certain targets of known spectral character were identifiable in the data. Correction from the remotely sensed spectral signature to some standard signature for a given target could indicate how the rest of the data should be corrected for atmospheric effects. An obvious extension of this idea would be to place a ground-truth team in the area at the time of overflight so that the true spectral character of a few targets could be measured under the actual conditions of remote-sensor data acquisition; later comparison of the ground data and airborne or satellite data would then provide true corrections for the actual atmospheric conditions existing at the time of the flight.

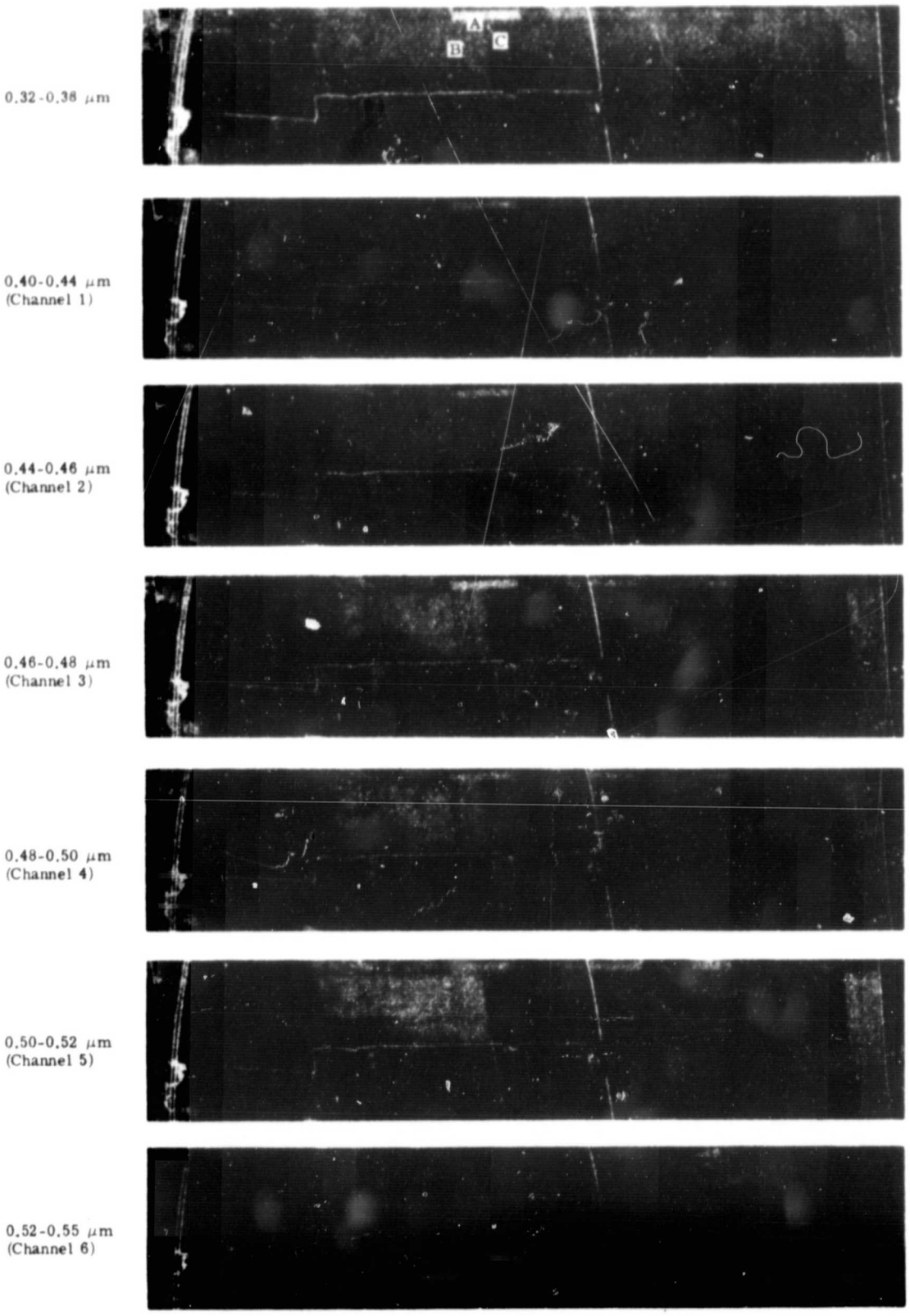

FIGURE 8. SCANNER IMAGERY TAKEN AT AN ALTITUDE OF 2000 FT. Data acquired at 0947 hours on 15 September 1966 near the Purdue University Agronomy Farm.

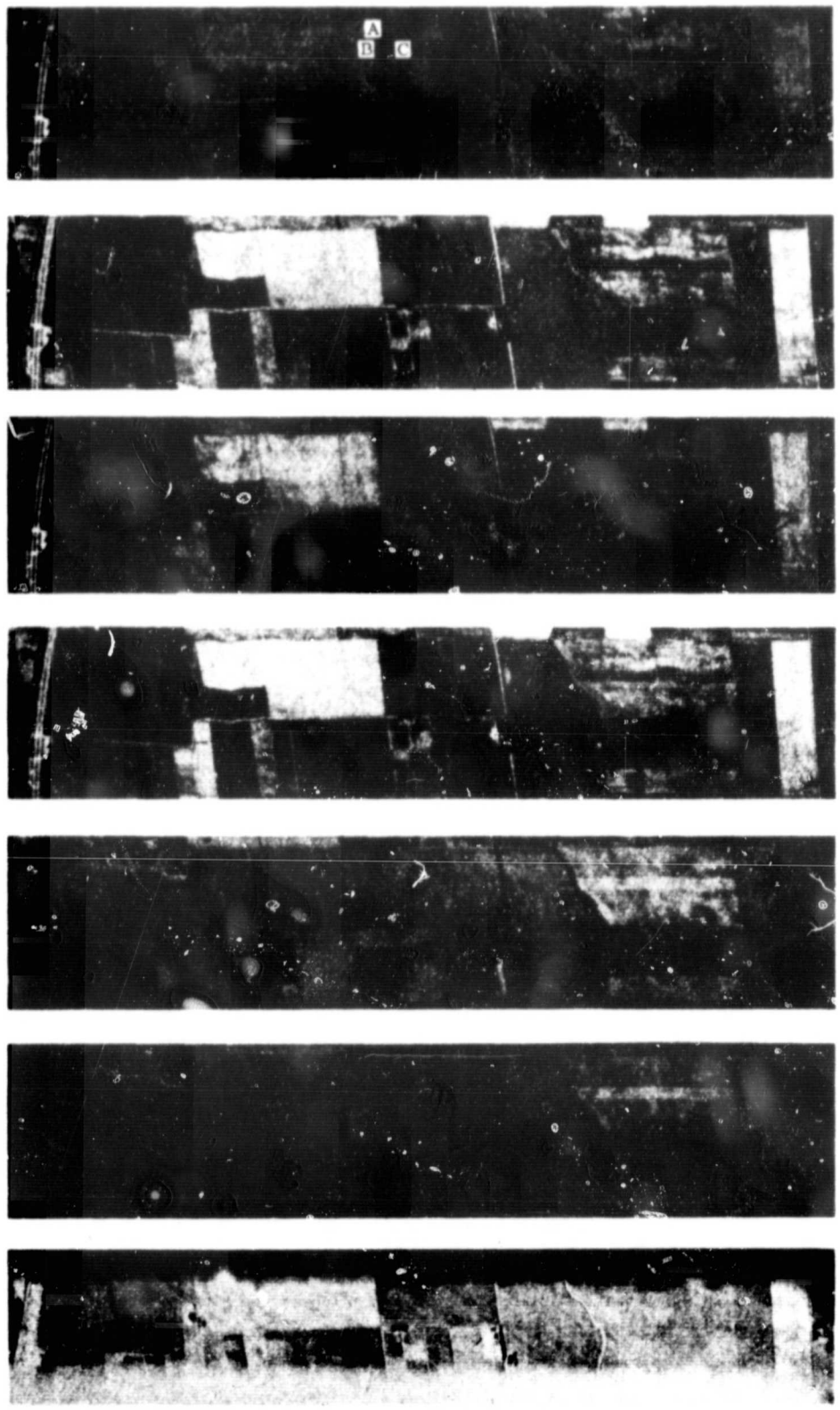

FIGURE 8. SCANNER IMAGERY TAKEN AT AN ALTITUDE OF 2000 FT (Continued)

0.32-0.38 μm

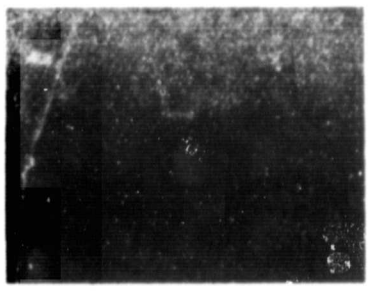

0.40-0.44 μm
(Channel 1)

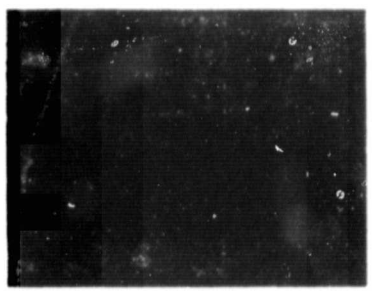

0.44-0.46 μm
(Channel 2)

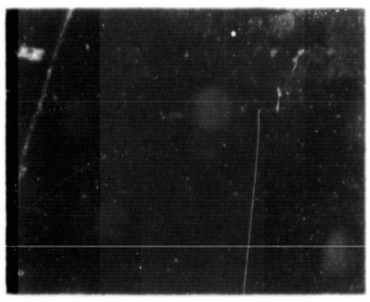

0.46-0.48 μm
(Channel 3)

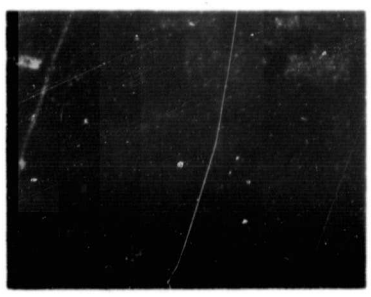

0.48-0.50 μm
(Channel 4)

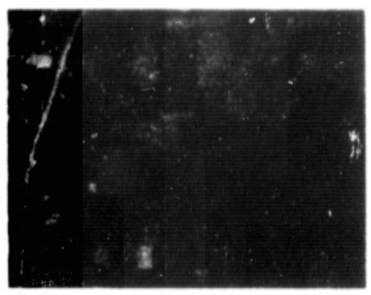

0.50-0.52 μm
(Channel 5)

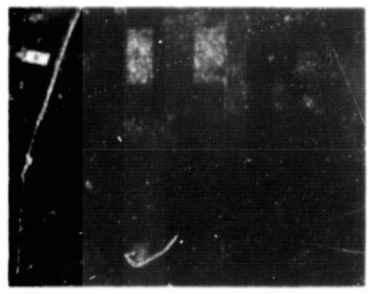

0.52-0.55 μm
(Channel 6)

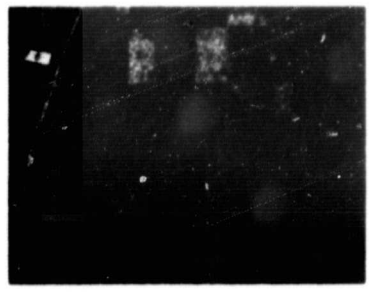

FIGURE 9. SCANNER IMAGERY TAKEN AT AN ALTITUDE OF 8000 FT. Data acquired at 0850 hours on 15 September 1966 near the Purdue University Agronomy Farm.

0.55-0.58 μm
(Channel 7)

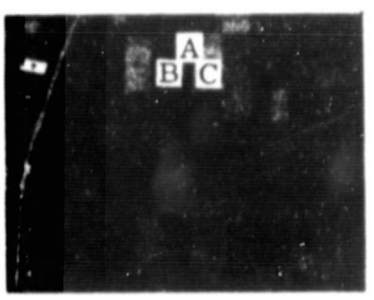

0.58-0.62 μm
(Channel 8)

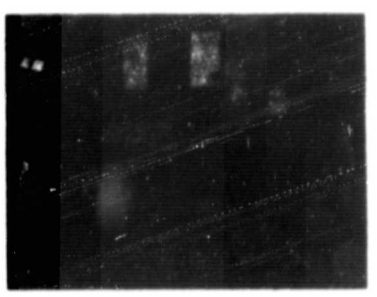

0.62-0.66 μm
(Channel 9)

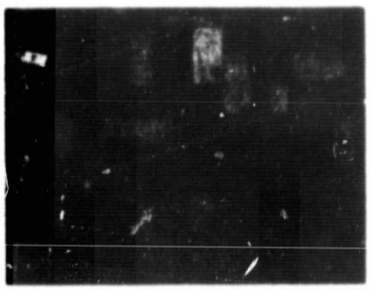

0.66-0.72 μm
(Channel 10)

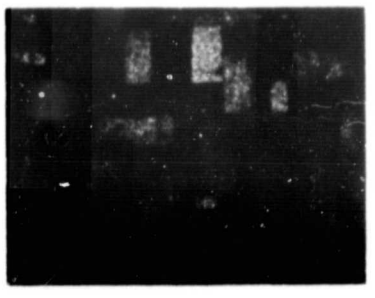

0.72-0.80 μm
(Channel 11)

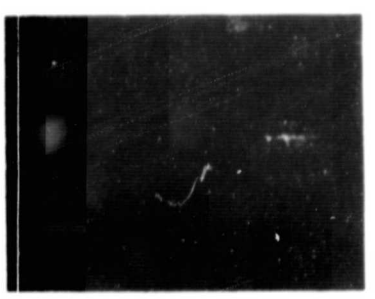

0.80-1.0 μm
(Channel 12)

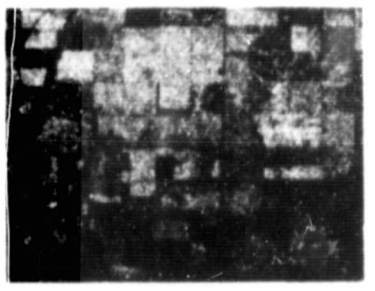

8.0-13.5 μm

FIGURE 9. SCANNER IMAGERY TAKEN AT AN ALTITUDE OF 8000 FT (Continued)

Appendix
INSTRUMENTATION AND CALIBRATION OF THE AIRBORNE MULTISPECTRAL SCANNER

The multichannel scanning system operated in a C-47 aircraft at Willow Run Laboratories obtains simultaneous imagery in as many as 18 discrete channels in the spectral range from 0.32 to 13.5 μm. In addition, four P-2 aerial cameras provide photographic data using Plus-X pan film, infrared aerographic film, normal color film, and camouflage-detection false-color film. The primary element of the system is a 12-channel spectrometer operating in the range from 0.4 to 1.0 μm. By employing a common aperture and prism dispersion to 12 photomultiplier detectors, truly instantaneous sensing of a given ground patch is achieved in 12 contiguous bands. In addition to the spectrometer, any three of the following detectors can be used at one time: a single-element detector operating at 0.32-0.38 μm; a three-element detector operating simultaneously at 1.0-1.4, 1.5-1.8, and 2.0-2.6 μm; a single-element detector operating 4.5-5.5 μm; and a single-element detector operating at 8.0-13.5 μm.

Calibration of the multispectral data is achieved using reference lamps and blackbody plates. The spectrometer and those detectors responsive to wavelengths of less than 2.6 μm are operated in one scanner housing which is equipped with two radiance-calibrated quartz-envelope tungsten filament lamps. During each scan, the field of view looks sequentially at 80 angular degrees of ground data, the two calibration lamps, and the dark interior of the scanner housing. The thermal detectors sensitive to wavelengths of more than 4.5 μm are normally operated in a second scanner housing. This housing is equipped with two temperature-controlled blackbody plates which are viewed sequentially with the ground scene, giving an apparent temperature calibration to the thermal imagery. Because of physical limitations on the positioning of these blackbody plates, the external angular field of view for imagery from this scanner is effectively limited to 35 degrees.

For the present investigation, data recorded by the 12-channel spectrometer were analyzed in the laboratory using electronic sampling techniques. Electronic gating was used to retrieve samples of the signal for a given ground patch simultaneously from each of the 12 channels. An area-averaged signal for a given target was obtained by taking ten discrete samples from various points on the target. Clamping of the zero voltage level to the zero radiance level represented by the interior of the scanner housing resulted in 12 average signal voltages which were proportional to the average apparent radiance of the target in each channel. Similar sampling of the two calibration lamp signals provided two additional voltages for each channel which were proportional to the known radiances of the lamps. The variation of output voltage with radiance could then be determined and the target signals calibrated in terms of apparent radiance at the aperture of the system.